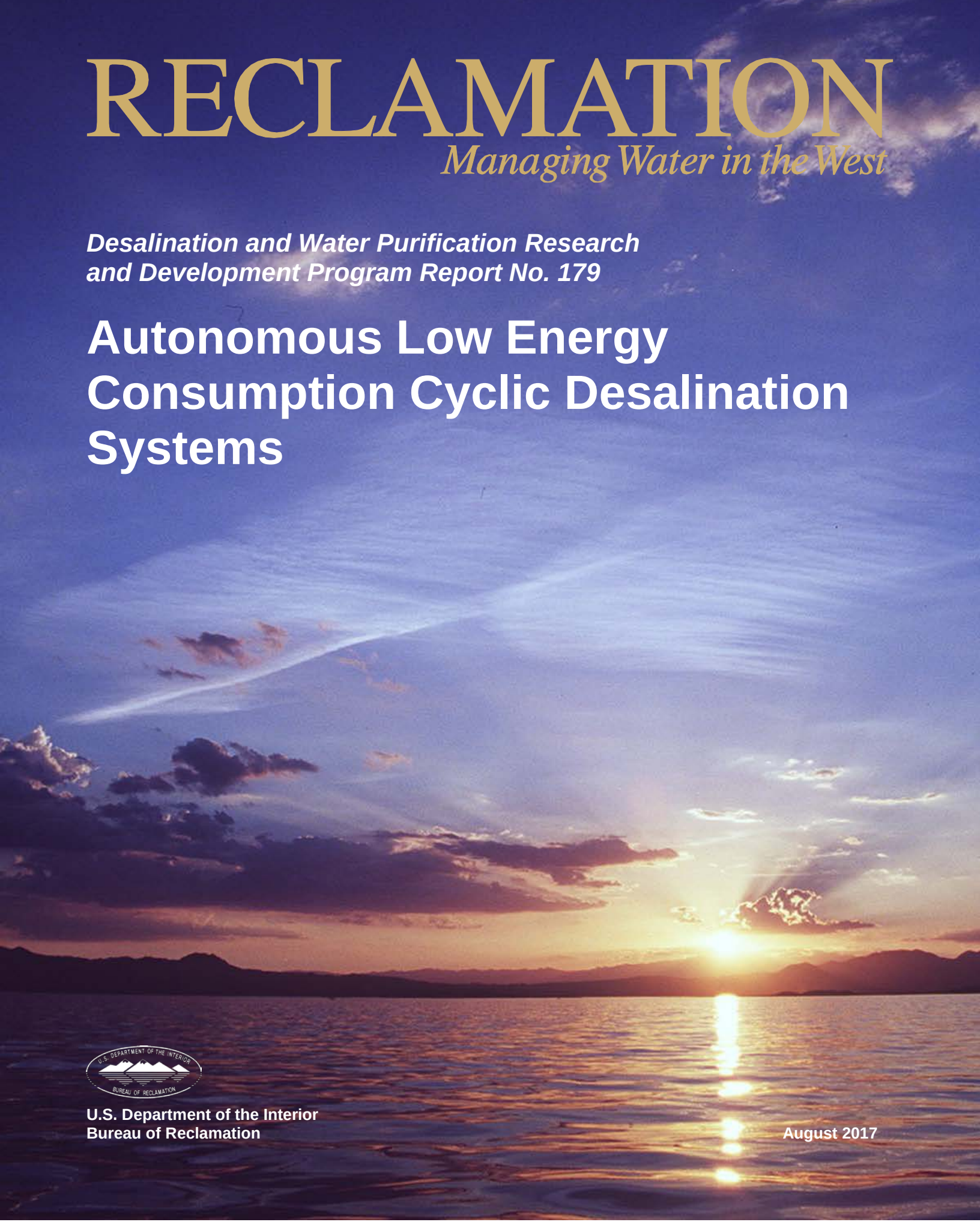

RECLAMATION

Managing Water in the West

Desalination and Water Purification Research and Development Program Report No. 179

Autonomous Low Energy Consumption Cyclic Desalination Systems

U.S. Department of the Interior
Bureau of Reclamation

August 2017

REPORT DOCUMENTATION PAGE	Form Approved OMB No. 0704-0188

PLEASE DO NOT RETURN YOUR FORM TO THE ABOVE ADDRESS.

1. REPORT DATE *(DD-MM-YYYY)*	2. REPORT TYPE	3. DATES COVERED *(From - To)*
August 17, 2017	Final Report	9/18/2013 - 9/30/2015

4. TITLE AND SUBTITLE
Autonomous Low Energy Consumption Cyclic Desalination Systems

5a. CONTRACT NUMBER

5b. GRANT NUMBER
R13AC80025

5c. PROGRAM ELEMENT NUMBER

6. AUTHOR(S)
Yoram Cohen
Anditya Rahardianto
Tae K. Lee

5d. PROJECT NUMBER

5e. TASK NUMBER

5f. WORK UNIT NUMBER

7. PERFORMING ORGANIZATION NAME(S) AND ADDRESS(ES)
The Regents of the University of California, Los Angeles
10889 Wilshire Blvd, Suite 700
Box 951406
Los Angeles, CA 90095-1406

8. PERFORMING ORGANIZATION REPORT NUMBER

9. SPONSORING/MONITORING AGENCY NAME(S) AND ADDRESS(ES)
Bureau of Reclamation, Department of the Interior
Denver Federal Center
PO Box 25007
Denver Colorado 80225-2007

10. SPONSOR/MONITOR'S ACRONYM(S)
Reclamation

11. SPONSOR/MONITOR'S REPORT NUMBER(S)

12. DISTRIBUTION/AVAILABILITY STATEMENT

13. SUPPLEMENTARY NOTES

14. ABSTRACT
We developed a new approach to autonomous CRO desalination: the University of California Los Angeles (UCLA) CRO. The present study involved theoretical model development, system construction, laboratory evaluation, and field deployment. In short, our analysis and experimental data shows that the claims that CRO is more efficient than conventional steady state RO are deficient. We show that because of dispersion, CRO may be more energy efficient that RO that is operated without an energy recovery device (ERD), but only in a limited range and only under ideal conditions. Steady state RO with energy recovery device will always be superior except when compared with an ideal CRO in which plug flow exists without dispersion (an impossibility in the real world).

On the other hand, the combination of steady state RO with partial recycle with the option of switching to CRO when needed (in both cases for high recovery and to maintain small footprint) would result in a highly flexible RO system that is ideal for distributed deployment. Given the successful proof-of-concept laboratory evaluation in the present study, an expanded pilot-scale evaluation of the present cyclic operational approach is recommended. Future studies should also quantify the balance between operational flexibility and energy consumption on the overall operational cost of CRO.

15. SUBJECT TERMS
Desalination, reverse osmosis, CRO operation, RO energy consumption, cyclic reverse osmosis

16. SECURITY CLASSIFICATION OF:			17. LIMITATION OF ABSTRACT	18. NUMBER OF PAGES	19a. NAME OF RESPONSIBLE PERSON
Unclassified					Saied Delagah
a. REPORT	b. ABSTRACT	a. THIS PAGE			19b. TELEPHONE NUMBER *(Include area code)*
U	U	U	SAR	50	303-445-2248

Desalination and Water Purification Research and Development Program Report No. 173

Autonomous Low Energy Consumption Cyclic Desalination Systems

Prepared for Reclamation Under Agreement No. R13AC80025
by

Yoram Cohen

Anditya Rahardianto

Tae K. Lee

U.S. Department of the Interior
Bureau of Reclamation
Technical Service Center
Water and Environmental Services Division
Water Treatment Engineering Research Team
Denver, Colorado

August 2017

MISSION STATEMENTS

The mission of the Department of the Interior is to protect and provide access to our Nation's natural and cultural heritage and honor our trust responsibilities to Indian tribes and our commitments to island communities.

The mission of the Bureau of Reclamation is to manage, develop, and protect water and related resources in an environmentally and economically sound manner in the interest of the American public.

Disclaimer

The views, analysis, recommendations, and conclusions in this report are those of the authors and do not represent official or unofficial policies or opinions of the United States Government, and the United States takes no position with regard to any findings, conclusions, or recommendations made. As such, mention of trade names or commercial products does not constitute their endorsement by the United States Government.

Acknowledgements

The project team acknowledges the contributions to the project by the Naval Facilities Engineering Command Engineering Service Center (NAFVAC ESC) at the Naval Base Ventura County (NBVC). In particular, the support of William Varnava and Timothy Petro is appreciated in field testing at the NAVFAC ESC Seawater Desalination Facility. Special thanks are also due to Michelle Chapman and Saied Delagah, Reclamation project managers, for their support and contributions to the project. The help of University of California Los Angeles (UCLA) undergraduate students Yeunha Kim and Yian Chen is also appreciated and acknowledged.

Contents

Figures

Tables

Abbreviations and Acronyms

CR	concentrate recycle system configuration
CRO	cyclic reverse osmosis
CW	concentrate withdrawal system configuration
ERD	energy recovery device
FT	filtration
FL	flushing
FT1	flow rate
FT2	product flow rate
M1	motor
M2	main pump motor
NAFVAC ESC	Naval Facilities Engineering Command Engineering Service Center
NF	nanofiltration
NBVC	Naval Base Ventura County
PAC	Process Automation Controller
PI	proportional-integral
RO	Reverse Osmosis
SSRO	steady state reverse osmosis
SEC	Specific energy consumption
TDS	total dissolved solids
tr	restriction
UCLA	University of California Los Angeles
UF	ultrafiltration

Measurements

GPD	gallon per day
GFD	gallon per square feet per day
GPM	gallon per minute
L	liter
L/min	liter per minute
mg/L	milligrams per liter
ppm	part per million
μm	micrometer

Variables

$\overline{c}$	average solute concentration within the element
c_f	RO feed concentration
c_c	RO concentrate salt concentration
$c^*_{c,ave,\infty}$	The time average RO concentrate salt concentration
$c_{c,hi}$	maximum allowable high limit of RO concentrate salt concentration
$c_{c,min}$	Minimum RO concentrate salt concentration in a cycle
$c_{c,max}$	Maximum RO concentrate salt concentration in a cycle
$C_{cMax,\infty}$	Need to define in Figure 7
cf	membrane unit feed solute concentration
c_o	RO raw feed solute concentration
c_p	RO permeate salt concentration
F(Θ)	Cumulative distribution function for RO retentate flushing
m_s	solute mass
η_{ER}	energy recovery device efficiency
η_{ERD}	concentrate energy recovery of efficiency of η_{ERD},
η_P	pump efficiency
NSEC	CRO SEC normalized with respect to the raw water osmotic pressure
o	raw feed stream
P	pressure (psi)
p	permeate stream
$p_{f,tr}$	applied pressure for RO operation
π	osmotic pressure
π_0	raw water osmotic pressure
q	volumetric flow rate
q_c	concentrate flow rate
q_f	RO module feed volumetric flow rates
q_o	raw system feed flow rate
q_p	RO module permeate volumetric flow rate
R_{nom}	R nominal salt rejection
ss	steady-state concentrate salt concentration
τ	Hydraulic residence time
t_{FT}	filtration duration
t_{FL}	flushing duration
Θ	Filtration/flushing duration relative to the residence time (Θ=t/τ)
V_e	RO element volume
V_m	volume of the recycle circuit
W_p	work during the filtration period
Y_m	RO module per-pass water recovery
Y_S	RO system instantaneous water recovery
Y_T	RO overall (cycle) system water recovery
$Y_{T,hi}$	overall water recovery limit
$Y_{T,use}$	overall product water recovery defined by the suer
$Y_{T,target}$	overall target product water recovery

Executive Summary

The research project focused on developing the fundamental scientific framework for analysis, optimization, and control of autonomous cyclic reverse osmosis (CRO) desalination processes. Reverse osmosis (RO) technology is now a mature technology for seawater and brackish water desalination, as well as for expanding applications in water reuse and contaminant removal. In contrast to conventional RO operated in steady-state, the CRO concept in the present study is based on transient operational strategy involving periodic switching between the modes of concentrate recycle for filtration and concentrate withdrawal for flushing. By using the CRO approach, water recovery can be independently varied through simple control of time-dependent concentration buildup in the RO retentate, which can be decoupled from control of permeate flux and retentate cross-flow velocity. In addition to high operational flexibility, recent theoretical work in the literature suggested potential energy benefits of CRO relative to conventional steady state RO. Nevertheless, much of existing theoretical work, in addition to lacking experimental verification, is based almost entirely on calculations of CRO specific energy consumption during the filtration period with minimal considerations of the impact of the RO flushing period. Furthermore, ideal plug flow is typically assumed in the assessment of RO retentate flushing (Qiu and Phillip 2012, Lin and Elimelech 2015, Warsinger et al. 2016, Efraty 2016, and Stover 2013), thereby neglecting the impact of longitudinal dispersion on the effectiveness of RO retentate flushing. Limited experimental analysis (Qui and Davies 2012), for example, have shown that ineffective RO retentate flushing can lead to build up of inter-cycle osmotic pressure and/or increase in the required flushing duration—affecting overall water recovery and specific energy consumption.

Accordingly, we developed a new approach to autonomous CRO desalination: the University of California Los Angeles (UCLA) CRO. The present study involved theoretical model development, system construction, laboratory evaluation, and field deployment. The model, verified by experimental data, revealed that flushing characteristics of the RO retentate module, particularly the impact of axial dispersion that lengthen the required flushing duration to achieve a given extent of flushing, has critical impact on the time average RO concentrate salt concentration and thus energy footprint of CRO. The present process model and experimental data indicated that operating with short flushing duration (at or slightly above the hydraulic residence time) and thus with inter-cycle salt accumulation is more energy-optimal than with complete flushing that necessitates operation with higher extents of intra-cycle salt accumulation. Using the model, a model-based control approach was proposed, allowing for automatic determination of the water recovery range of CRO based on real-time raw feed water salinity data.

Given energy-optimal CRO operation, it was shown that the potential energy benefits of CRO (as suggested in the literature referenced above) is only achievable under ideal plug flow condition in the RO retentate stream during flushing, which is difficult to achieve in practical RO systems. Analysis based on realistic theoretical (laminar flow in pipe or rectangular channel) and experimental flushing conditions (based on the UCLA system) revealed that the specific energy consumption of CRO is likely to be higher than that of steady-state RO with energy recovery. Nevertheless, the challenge of higher energy consumption of CRO under realistic field condition (relative to steady state RO with energy recovery) is likely to be overcome by the benefit of high operational flexibility of CRO to operate over a wide range of water recovery levels using a single system platform. Given the successful proof-of-concept laboratory evaluation in the present study, an expanded pilot-scale evaluation of the present cyclic operational approach is recommended. Future studies should also quantify the balance between operational flexibility and energy consumption on the overall operational cost of CRO.

1. Background

1.1. Introduction

Reverse osmosis (RO) has emerged as the dominant desalination technology primarily due to its relative simplicity, compactness, modularity, and scalability (Greenlee 2009 and Gray 2011). RO water production is pressure driven, avoiding the complexity, relatively higher energy use, and higher capital costs of osmotically- or heat-driven desalination processes (i.e., forward osmosis, membrane distillation, solar evaporation) (Camacho 2013 and Shaffer 2014). In fact, osmotically-driven (with thermolytic draw solutions) and heat-driven desalination processes are cost-effective only if low-cost heat sources (or "waste heat") are readily available locally (Camacho 2013 and Shaffer 2014). As pressure-driven RO desalination uses electrical energy for pressure generation, RO has significant deployment flexibility for harnessing renewable energy (e.g., via solar photovoltaic cells and wind turbine), while maintaining consistent operability through the conventional power grid as backup power (Ghermandi and Messalem 2009 and GE Global Research 2006). Various approaches to reducing RO energy consumption are also well established, such as using energy recovery devices and staged operation with booster pumps (Zhu et al. 2009 and 2010). RO desalination technologies have been commercially successful for decades. Indeed, RO desalination operations and maintenance are now well supported by diverse and well-established supply chain of off-the-shelf components and consumables (membrane elements, prefilters, compatible antiscalants, etc.).

While RO desalination is a well-established technology, the relative operational inflexibility of conventional RO systems remains a major challenge. Conventional RO systems designed for seawater desalination, for example, typically cannot be operated optimally for brackish water desalination and vice versa. This is because conventional RO systems, which commonly operate in a steady-state mode, must be tailored to handle specific water sources, requiring a relatively high degree of customization. Under conventional RO/nanofiltration (NF) design principles, a target water recovery is first selected based on a source-specific water composition and salinity (Greenlee et al. 2009 and McCool et al. 2010). A fixed number of RO/NF elements in a specific serial arrangement of (Figure 1a) are then specified to meet the selected target water recovery.

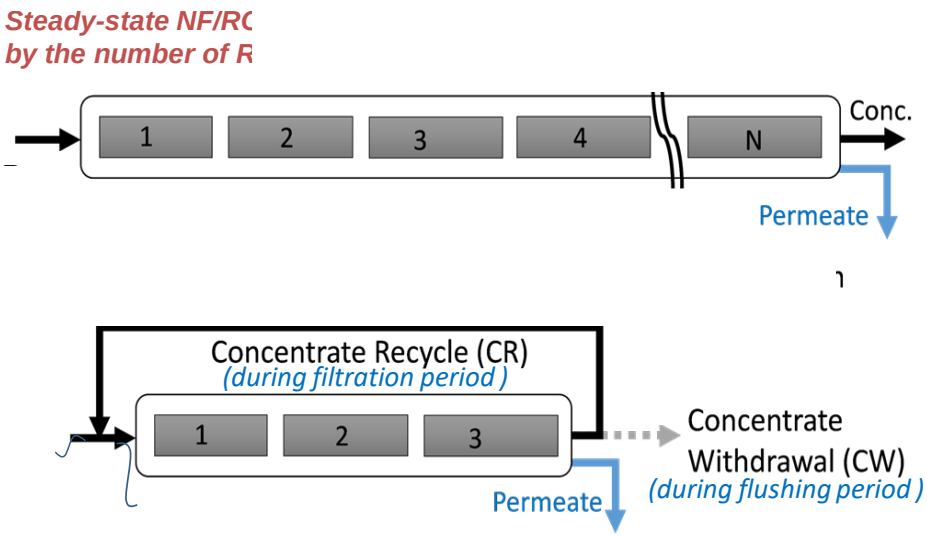

Figure 1. Comparison of RO systems operating in a conventional steady-state and cyclic modes.

This steady-state arrangement requires careful selection of appropriate membranes, design target permeate flux, and minimum retentate cross-flow velocity to balance the following factors, based on Rahardianto et al. (2006), Rahardianto et al. (2007), and Thompson et al. (2013):

(a) meeting product water quality targets

(b) maximizing membrane productivity (i.e., system foot-print)

(c) minimizing energy consumption

(d) reducing the potential for membrane fouling/mineral scaling .

Maintaining the above intricate balance is challenging in conventional RO operation because water recovery, permeate flux, and cross-flow velocity are highly coupled (Gao et al. 2013), limiting operational flexibility and requiring significant operational and design expertise and/or sophisticated process control.

In the past decade, transient CRO operation has been advanced based on early proposed concepts by Bratt (1989) and Szucz and Szucz (1991) in the late 80s and early 90s as an approach for addressing the lack of operational flexibility of conventional steady-state RO operation (Davies 2011, Efraty 2012, Efraty et al. 2011, and Qiu et al. 2012). Cyclic RO systems rely on transient semi-batch RO operation in which system configuration is alternated, in a timed cyclical manner, between a full RO concentrate recycle during the filtration period (Figure 1b) and a conventional RO configuration (Figure 1a) for periodic RO concentrate withdrawal during the RO module flushing period (Figure 1b). In each cycle, water production occurs primarily during the filtration period; water production loss due to concentrate withdrawal only occurs during the short flushing period.

Thus, the overall product water recovery per cycle (i.e., ratio of product to raw feed water volumes over a cycle) is also governed by the relative duration of the filtration and flushing periods. Compared to conventional RO, the relative duration of the filtration-flushing periods in CRO provides an additional degree of freedom (i.e., becomes an independent variable) to decouple the control of water recovery from that of permeate flux and cross-flow velocity, thereby enhancing the operational flexibility of the RO process.

In addition to enhanced operational flexibility, recent work (Qiu et al. 2012 [configurations], Lin and Elimelech 2015, Warsinger et al. 2016, and Stover 2012) have conjectured that cyclic semi-batch RO operations may be more energy efficient than conventional steady-state RO. This has been typically based on the expectation of potentially lower levels of transient RO feed pressure and raw feed flow rate in cyclic semi-batch RO operation relative to the constant, steady-state pressure and raw feed flow rate in conventional RO, respectively. Specifically, conventional RO operates at a steady-state where the RO concentrate salt concentration and thus osmotic pressure are both time-invariant (with respect to constant feed salinity) and depend on the level of set product water recovery. In contrast, CRO operates with dynamically varying RO concentrate salt concentration that should ideally be kept at levels no higher than the steady-state value in conventional RO.

In CRO, a cycle begins with a filtration period in which the entire RO concentrate is recycled back to the RO feed. In this mode, the product water is produced at the same volumetric flow rate as the incoming raw feed water flow rate, setting the instantaneous water recovery to 100 percent. However, since membrane salt rejection leads to transient osmotic pressure build-up in the RO retentate recycle circuit, a corresponding transient increase in the RO feed pressure is required to maintain the target water productivity. Unlike conventional RO, the CRO feed pressure is pegged with the dynamically-changing RO retentate osmotic pressure. The period of water production continues in the filtration period until the RO retentate concentration reaches a given threshold level. Subsequently, a short flushing period is actuated to discharge the concentrate from the RO module using the raw RO feed. This step is actuated to reduce the osmotic pressure and prepare the system for a new CR period in the succeeding cycle. In conventional RO, the raw feed flow must always be pressurized, but in CRO, the raw feed flow may be greater than the product flow only during the short flushing periods (if the RO elements are pressurized during the flushing period). Thus, the energy needed to pressurize the raw feed flow is less in CRO than in conventional RO. Thus, in principle, the conjecture that CRO may achieve lower specific energy consumption than conventional RO should only be realizable under ideal conditions that lead to lower average transient feed pressure (relative to steady state RO) and sufficiently short flushing periods.

Given the potential for energy use reduction in CRO operation, recent studies have focused on comparing the theoretical minimum specific energy consumption

(i.e., energy consumed per unit volume of product water) of CRO to conventional RO. For example, Qui et al. (2012) derived the theoretical minimum energy footprint for CRO process operating at the limit of crossflow thermodynamic restriction. The above study reported predictions of substantially lower minimum specific energy consumption for CRO than conventional single-stage RO. Similar theoretical analysis by Lin and Elimelech 2015 also appear to be consistent with the above earlier studies. It is stressed, however, that the previous theoretical studies did not provide experimental verification of the claims of reduced SEC and based their analyses entirely on calculations of CRO specific energy consumption during the filtration period with insufficient considerations of the impact of the RO flushing period. Furthermore, previous studies have based their analysis of CRO on the assumption of ideal plug flow in the assessment of RO retentate flushing (Qiu and Phillip 2012, Lin and Elimelech 2015, Warsinger et al. 2016, Efraty 2016, and Stover 2013), thereby neglecting the impact of longitudinal dispersion on the effectiveness of RO retentate flushing. Limited experimental analysis Qiu, T.Y. and P.A. Davies, 2012 (Batch), for example, has shown that ineffective RO retentate flushing can lead to build up of inter-cycle osmotic pressure and/or increase in the required flushing duration, affecting overall water recovery and the process' specific energy consumption (SEC). To better assess energy footprint of CRO under realistic conditions, a fundamental process modeling framework is needed to account for the effect of longitudinal dispersion during the flushing periods of CRO on inter-cycle osmotic pressure buildup.

In addition to their potential for minimizing energy consumption, if feasible, CRO systems should operate autonomously to effectively take advantage of the potential high operational flexibility. Given the dynamic nature of the CRO process, robust and self-adaptive system operation will require advanced process control to optimally handle variations in feed water conditions, as well as optimal operation with respect to energy cost and availability. In recent years, advanced model-based self-adaptive control of steady-state RO processes was shown to enable SEC reduction (Bartman et al. 2009 (non-linear), Bartman et al 2009 (feed flow), and Bartman et al 2010). A similar basic framework for model-based control of CRO processes can in principle be developed, but this framework will require accurate cyclic process model that includes both the filtration and concentrate discharge periods.

1.2. Project Overview

In order to evaluate the potential operational flexibility and energy savings of CRO, the goal of the proposed project was to develop the fundamental scientific framework for analysis, optimization, and control of CRO desalination processes. Toward this goal, the objectives of the proposed project were to:

(a) Develop CRO process models of CRO system and controller design and process analysis

(b) Develop a model-based controller for autonomous CRO operational control

(c) Retrofit a laboratory spiral-wound RO system to enable experimental evaluation of autonomous CRO operation

(d) Conduct an experimental study to validate the developed CRO process models

(e) Implement a proof-of-concept laboratory demonstration of extended, multi-cycle autonomous CRO operation

The project was organized along the 5 tasks summarized below.

- ***Task 1: Process Modeling & Simulation of Cyclic RO Desalination Process.*** Development of process modeling framework for CRO process (Subtask 1.1), simulation and optimization of CRO process operational strategies (Subtask 1.2), are described in Section 2. *Cyclic Process Modeling and Analysis.* Cyclic RO model verification (Subtask 1.3) and comparison of Cyclic RO versus conventional steady-state RO (Subtask 1.4) are presented in Sections 4.2. *Cyclic RO Operation over Multiple Cycles* and 4.3. *Determination of CRO System Flushing Characteristics.*

- ***Task 2: Retrofitting of Laboratory Spiral Wound RO System to Enable Cyclic Operation.*** Retrofit system design and component selection (Subtask 2.1), acquisition of system components (Subtask 2.2) and retrofit system construction (Subtask 2.3) were accomplished with the development of the UCLA laboratory system as described in Section 4.1. *Evaluation of Cyclic RO Operation.*

- ***Task 3: Design & Implementation of Cyclic RO Process Controller.*** The design of CRO process automation controller (Subtask 3.1) are presented in Section 4.7. The controller implementation (Subtask 3.2) was tested as described in Sections 4.2. *Cyclic RO Operation over Multiple Cycles* and 4.4. *Field Demonstration of CRO Operation.*

- ***Task 4: Laboratory Evaluation of Autonomous Cyclic RO Operation.*** Autonomous CRO operations over extended cycles (Subtask 4.2) and of CRO process robustness (Subtask 4.3), along with evaluation of process performance and energy consumption (Subtask 4.3) were first evaluated in the laboratory as described in Sections 3.3. *Cyclic RO System Operation, 5.4. Determination of CRO System Flushing Characteristics* and 4. *Results and Discussion.* Extensive evaluations in the field are described in Sections 3.3. *Cyclic RO System Operation* and. 4.4. *Field Demonstration of CRO Operation.*

- ***Task 5: Reporting.*** Quarterly progress reports were prepared and submitted to the Bureau of Reclamation (Reclamation). The project was completed with the submission of this final report.

1.3. Conclusions and Recommendations

We developed a new approach to autonomous CRO desalination in the present study and demonstrated it through theoretical model development, UCLA CRO system construction, laboratory evaluation, and field deployment. The developed CRO process model enabled characterization of the alternating filtration and flushing periods of CRO. We validated the model using experimental data revealing that the flushing (i.e., concentrate discharge) characteristics of the RO retentate module, particularly the impact of axial dispersion, affected the length of the flushing duration required to achieve the targeted level of concentrate discharge. The extent of concentrate flushing was found to have a critical impact on the time average RO concentrate salt concentration in the RO system and thus the CRO's energy footprint. Because solutes disperse during the RO element, short flushing duration leads to incomplete flushing and thus inter-cycle salt accumulation, which elevates the stable minimum and maximum RO salt concentration in multiple-cycle operations. On the other hand, increasing the flushing duration to achieve complete extent of flushing requires increased filtration duration to maintain the same overall cycle water recovery and thus higher extent of intra-cycle salt accumulation. It was shown that the average RO concentrate salt concentration is more sensitive to intra- than inter-cycle salt accumulation. The present process model and experimental data indicated that operating with a short flushing duration (at or slightly above the hydraulic residence time) and thus with inter-cycle salt accumulation is more energy-optimal than with complete flushing that requires operating with higher extents of intra-cycle salt accumulation.

Given that raw feed water salinity varies temporally in most practical applications, a self-adaptive operational approach is important for effective CRO operation. Therefore, we developed a model-based control which allowed for determination of the water recovery range of the CRO process based on real-time raw feed water salinity data. Such an approach, which we demonstrated in a field study, enabled determination and implementation of energy-optimal filtration and flushing durations during CRO operation which was evaluated.

CRO process analysis that considered salt dispersion during the flushing period revealed that the SEC (in kwh/1,000 gal) for CRO would be lower than steady state RO only if the flushing process is ideal under plug flow conditions. However, when more realistic salt dispersion is considered in the analysis of the flushing period, the SEC for the CRO would be higher than for a single stage steady-state RO with energy recovery. Moreover, CRO has the benefit of high

operational flexibility over a wide range of water recovery levels with a single system platform. Given the above findings, it is reasonable to suggest that expanded pilot-scale evaluation of the present operational approach to CRO should focus on quantifying the balance between operational flexibility and energy consumption as well as the development of RO system designs that allow real-time switching of between steady state and CRO operation.

2. Cyclic Process Modeling and Analysis

2.1. Overview

In developing process models for CRO desalination, we considered a two-step cyclic process, with each cycle consisting of successive periods of RO membrane filtration (FT) and RO retentate flushing (FL). During the FT period, the system is configured for concentrate recycle such that the entire concentrate stream is continuously mixed with incoming raw feed stream and recycled as RO feed (Figure 2a). During the FT period (with flushing duration [t_{FT}]), the RO permeate is produced at the same volumetric flow rate as the incoming raw feed water. Membrane salt rejection leads to salt accumulation in the RO concentrate recycle stream, leading to a monotonic increase of RO concentrate salt concentration (cc) with time from the minimum ($cc_{,min},n$) to the maximum ($cc_{,max},n$) concentration values for a given cycle n (e.g., Figure 2). To complete the cycle, the flushing (FL) period is initiated by switching the system configuration to a concentrate withdrawal mode, enabling flushing of the RO system (element and other related components) with the raw feed water (Figure 2b) for a given duration (t_{FL}). During flushing, the RO concentrate salt concentration declines to a level that depends on the effectiveness and duration of concentrate flushing, establishing the initial condition for the next adjacent cycle ($c_{c,min,n+1}$) (Figure 2).

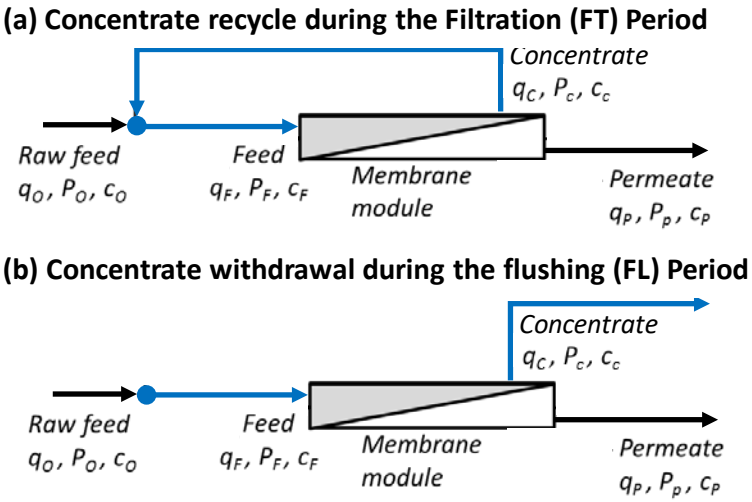

Figure 2. Concentrate recycle (CR) and concentrate withdrawal (CW) operational modes of CRO operation.

In multi-cycle RO operation (Figure 2), the first cycle typically starts from a steady-state RO operating condition at the RO module water recovery (defined as $Y_m=q_p/q_f$, where q_p and q_f are the RO module permeate and feed volumetric flow rates, respectively). The initial RO concentrate salt concentration ($c_{c,min,}1$) is therefore given by the steady-state concentrate salt concentration ($c_{c,ss}$) of the RO system operated at Y_m in the conventional configuration (i.e., Figure 2b), which can be deduced from steady-state solute mass balance as Equation 1:

Equation 1:

$$c_{c,ss} = \frac{1-(1-R_{nom})\cdot Y_m}{1-Y_m}$$

where:

$R_{nom} = 1 - c_P / c_o$ is the nominal salt rejection

where:

c_o is the RO raw feed concentration
c_p is the RO permeate salt concentration

Upon completion of the filtration period in each cycle, complete flushing should limit salt accumulation to occur only within each cycle (during the filtration period) with negligible inter-cycle salt accumulation. In this ideal case, the minimum RO concentrate salt concentration in CRO ($c_{c,min,n}$) is expected to closely approach the steady-state RO concentrate salt concentration ($c_{c,ss}$). Inter-cycle salt accumulation can occur due to incomplete flushing, leading to evolving levels of $c_{c,min,n}$ and $c_{c,max,n}$ with increasing number of cycles (Figure 3 and Figure 4). Both $c_{c,min,n}$ and $c_{c,max,n}$ can eventually reach stable values (with increasing n) as the rate of salt accumulation during the FT period is balanced by that of salt decumulation during the FL period. When flushing is incomplete, the stable level of RO concentrate salt concentration ($c_{c,min,\infty}$), would higher be than the steady-state RO concentrate salt concentration ($c_{c,ss}$; Figure 3 and Figure 4). This condition will lead to higher osmotic pressure and thus increase the instantaneous specific energy consumption. Process modeling of both intra-cycle (i.e., during the filtration period) and inter-cycle (i.e., as affected by flushing effectiveness) salt accumulations is therefore critical in analyzing CRO processes.

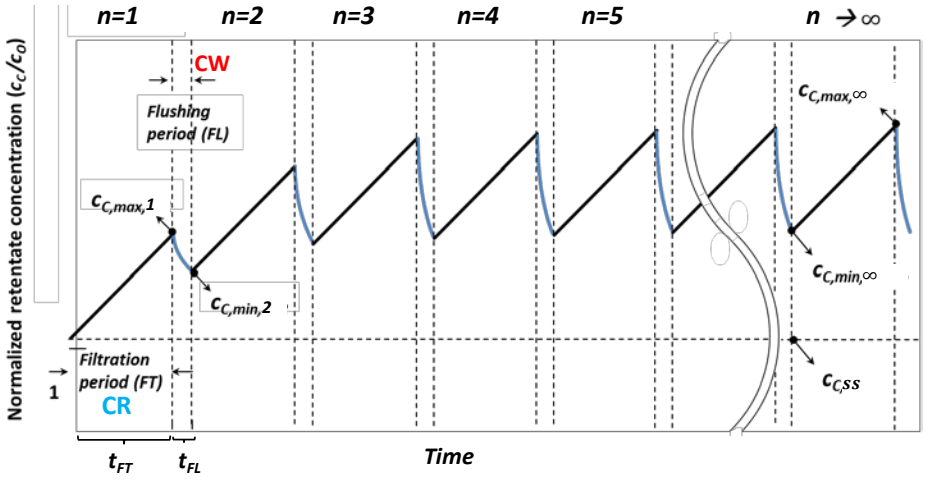

Figure 3. Time evolution of RO retentate concentration in multi-cycle operation of CRO.

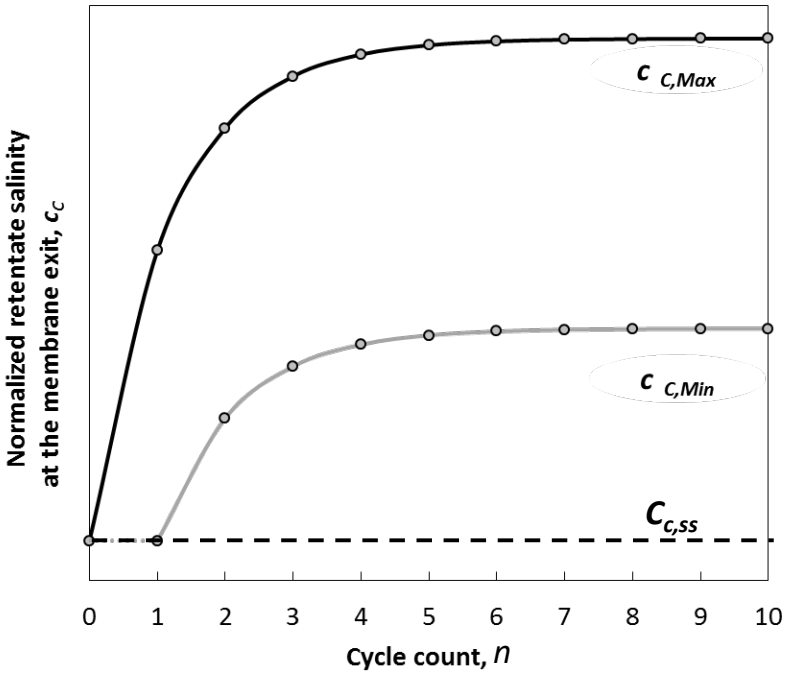

Figure 4. Illustration of the expected evolutions of the minimum and maximum RO concentrate salt concentration with increasing number of cycles.

Intra- and inter-cycle salt accumulations in CRO processes are considered in Sections 2.2. *CRO Filtration Pperiod* through Section 2.5. *Range and Time for Average RO Concentrate Salt Concentrations* where the retentate concentration profiles are evaluated during the filtration (i.e., concentrate recycle) and flushing (i.e., concentrate withdrawal) periods. The analysis is geared toward determining the cycle minimum and maximum retentate salt concentrations (i.e., cc,$_{min,n}$ and cc,$_{max,n}$). The dependence of cc,$_{min,n}$ and cc,$_{max,n}$ on product water recovery and their impacts on the theoretical minimum specific energy consumption (SEC) for

CRO are then considered. Subsequently, a model-based control approach for optimal CRO operation is presented.

2.2. CRO Filtration Period

During the filtration (FT) period of CRO, the entire concentrate stream (*c*) is continuously recycled and mixed with the raw feed water (*o*) as shown in Figure 2a. The volumetric rate of the RO feed stream is thus the sum of the raw feed and concentrate streams ($q_f = q_o + q_c$). Because the entire concentrate stream is recycled, the raw feed water is supplied to the membrane module at a volumetric flow rate equivalent to the permeate production rate ($q_o=q_p$). The instantaneous system water recovery (Y_S) ($Y_s=q_p/q_o$), which is the ratio of product water volume recovered from the raw feed stream, is therefore 100 percent during the FT period. Note that the per-pass water recovery through the RO membrane module (Y_m) (i.e., water recovered from RO feed, $Y_m=q_p/q_f$) is always smaller than the overall system water recovery during the FT period (i.e., $Y_s<Y_m$).

As product water is recovered from the RO feed stream (at a recovery of $Y_m=q_p/q_f$) at every pass through the RO module, cross-flow desalting leads to a solute concentration profile developing along the axial flow direction. Because concentrate is not withdrawn from the system, solute mass (m_s) accumulates in the RO retentate recycle circuit throughout the FT period (i.e., RO feed, RO module retentate channel, and RO recycle stream; see Figure 2a) at a rate that is equal to the difference in solute mass inlet flow from the raw feed stream (*o*) and solute mass passage through the membrane into the permeate stream (*p*) in Equation 2

Equation 2:

$$\frac{dm_s}{dt} = q_o c_o - q_p c_p$$

where:

q_o and q_p are the volumetric flow rates
c_o and c_p are corresponding solute concentrations in the raw RO feed (*o*) and RO permeate (*p*) streams, respectively.

As salt slowly accumulates in the RO concentrate recycle circuit, the axial retentate concentration profile (which is established quickly at each time step) is expected to slowly shift upwards. The rates of change of solute mass within the CRO system and within the RO element are equal and thus the following equality holds in Equation 3:

Equation 3:

$$\frac{V_e \cdot d\overline{c}}{dt} = \frac{dm_s}{dt}$$

where:

m_s is the solute mass in the CRO circuit
V_e is the RO element volume
$\overline{c}$ is the average solute concentration within the element

It reasonable to expect that the rate of change (with respect to time) of the average solute concentration in the element would approximately follow that of the concentration at the element exit (i.e., $d\overline{c} / dt \approx dc_c / dt$) . Therefore, combining Equations 2 and 3, noting that $q_o = q_p$, and for the special case where the volume of the recycle circuit (V_m) is primarily that of the membrane module ($V_m \approx V_c$), the RO concentrate salt concentration during the FT period can be described by Equation 4.

Equation 4:

$$\frac{dc_c}{dt} \approx \frac{q_{f,FT}}{V_m} \cdot \frac{q_p}{q_{f,FT}} \cdot \left(c_o - c_p\right) = \frac{q_{f,FT}}{V_m} \cdot c_o \cdot Y_m \cdot R_{nom}$$

Where:

$R_{nom} = 1 - c_P / c_o$ is the nominal salt rejection

$q_{f,FT}$ is the RO feed flow rate during the FT period.

Equation 5 provides the solution of the above differential equation given an initial concentrate salt concentration of a given cycle ($c_{c,\min}$) and assuming complete salt rejection ($R_{nom} \approx 1$):

Equation 5:

$$c_{c,n}\left(t\right) = Y_m \cdot R_{nom} \cdot c_o \cdot \frac{t}{\tau_{FT}} + c_{c,\min,n}$$

where:

$\tau_{FT} = V_m / q_{f,FT}$ is the hydraulic residence time in the RO module.

Equation 5 indicates that, during the filtration period, the RO concentrate salt concentration increases linearly with time from the cycle initial value ($c_{c,min}$) at a rate that depends on Y_m, τ_{FT} , and R_{nom}. The maximum RO concentrate salt concentration for a cycle n ($c_{c,max,n}$) is therefore given by Equation 6:

Equation 6:

$$c_{c,\max,n} = Y_m \cdot R_{nom} \cdot c_o \cdot \frac{t_{FT}}{\tau_{FT}} + c_{c,\min,n}$$

where:

t_{FT} is the filtration duration
$c_{c,min,1}$ is given by Equation 1

The subsequent value of $c_{c,min,n}$ depends on the effectiveness of the flushing process in each cycle.

2.3. CRO Flushing Period

To complete a cycle *n*, a flushing process needs to be implemented at the end of the filtration period. This is done to flush the concentrated brine out of the recycle circuit using raw feed water. Therefore, a new initial condition (i.e., $c_{c,min,n+1}$) is established that should enable implementation of a new filtration period in the subsequent cycle *n+1*. Implementing flushing involves rearranging the system to the conventional RO configuration (Figure 3b), whereby the RO module is fed with raw feed water (q_o=q_f) and, instead of recycling, the RO concentrate is discharged. The immediate change in system configuration thus leads to a negative step input change in the RO feed concentration at the end of each filtration process (i.e., after a given filtration duration, t_{FT}) in which $c_f = c_{f,\max}$ at the end of the filtration period and $c_f = c_o$ over the entire flushing period (Figure 5). Given a negative step input in the RO feed salt concentration at the initiation of the flushing process, a step response function $F(\Theta)$ can be defined based the RO concentrate salt concentration. Accordingly, the fraction of solute mass that is flushed out of the recycle circuit can be expressed as Equation 7:

Equation 7:

$$F(\Theta) = \frac{c_{c,\max,n} - c_{c,\min,n+1}}{c_{c,\max,n} - c_{c,ss}}$$

where:

$\Theta = t_{FL}/\tau_{FL}$ is the normalized flushing duration

The steady state RO concentrate salt concentration ($c_{c,ss}$) is theoretically reached when an infinite time is allowed for flushing. Combining Equation 6 and Equation 7 yields Equation 8 for predicting the minimum RO concentrate salt concentration of cycle *n+1* based on cycle *n* conditions:

Equation 8:

$$c_{c,\min,n+1} = \left(1 - F\left(\Theta\right)\right) \cdot \left(Y_m \cdot R_{nom} \cdot c_o \cdot \frac{t_{FT}}{\tau_{FT}} + c_{c,\min,n} \right) + c_{c,ss} \cdot F\left(\Theta\right)$$

where:

$c_{c,\min,1} = c_{c,ss}$ as given by Equation 1.

Examination of Equation 8 reveals that complete flushing ($F_n(\Theta) \approx 1$) would allow CRO to operate close to the steady-state RO concentrate salinity at the beginning of each cycle ($c_{c,\min,n+1} \approx c_{c,ss}$), if salt accumulation within the recycle circuit is limited to that of intra-cycle. In contrast, incomplete flushing ($F_n(\Theta) < 1$) leads to a minimum RO concentrate salt concentration in each cycle after n=1 to be greater than the steady state concentration ($c_{c,\min,n+1} \geq c_{c,\min,n} > c_{c,ss}$) due to inter-cycle salt accumulation. In principle, flushing under ideal plug flow conditions would reach completion ($F(\Theta) \approx 1$) as soon as the flushing duration reaches the hydraulic residence time ($\Theta = 1$). Axial dispersion, however, is expected to occur during flushing of RO modules. Thus, in practice, flushing duration longer than the hydraulic residence time ($\Theta > 1$) would be required to approach complete flushing.

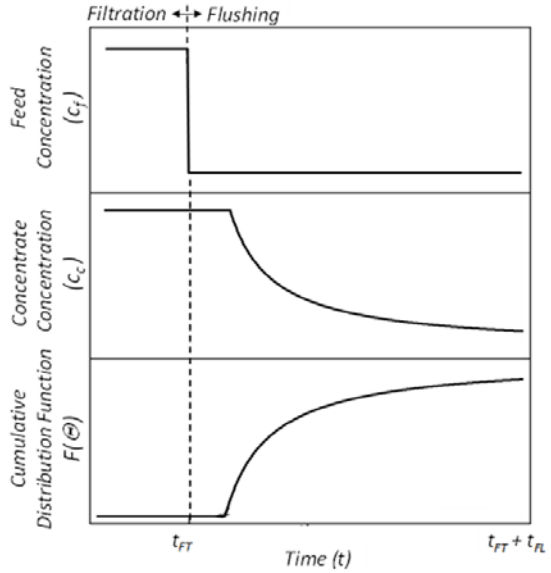

Figure 5. Illustrations of (a) a negative step change in the membrane unit feed solute concentration (cf), (b) the resulting decrease in the RO concentrate salt concentration (cc), and (c) the corresponding cumulative distribution function predicted

2.4. Cyclic RO Overall Product Water Recovery

Alternating the RO system configuration between total concentrate recycle and concentrate withdrawal during the filtration and flushing periods (Figure 2), respectively, would lead to the instantaneous system water recovery ($Y_S = q_p/q_o$) of CRO alternate between Y_S=100% (i.e., total recycle) during filtration and a lower value during flushing (equivalent to the module RO recovery, i.e., at $Y_S=Y_m$). Given the transient nature of the CRO process, the overall product water recovery (Y_T) must be defined for the entire cycle duration ($t_{FT}+t_{FL}$) based on the total product volume produced relative to that of the raw feed input used as shown in Equation 9:

Equation 9:

$$Y_T \equiv \frac{\text{Total permeate production}}{\text{Total raw feed input}} = \frac{q_{p,FT}\cdot t_{FT} + \delta \cdot q_{p,FL}\cdot t_{FL}}{q_{o,FT}\cdot t_{FT} + q_{o,FL}\cdot t_{FL}}$$

where:

δ=1 indicates pressurized flushing in which RO permeate production is maintained at $q_{p,FL}$
δ =0 is for low pressure flushing without permeate production

Assuming a simple CRO operation in which the water production and RO module feed flow rates are fixed ($q_{p,FT} = q_{p,FL}$ and $q_{f,FT} = q_{f,FL}$) and recognizing that $q_{o,FT} = q_{p,FT}$ during filtration, Equation 9 simplifies to the relationship shown in Equation 10:

Equation 10:

$$Y_T = \frac{Y_m\left(t_{FT}/t_{FL}\right) + \delta \cdot Y_m}{Y_m\left(t_{FT}/t_{FL}\right) + 1}$$

which indicates that, for a given module RO recovery, the overall product water recovery is fixed by the filtration duration relative to that of flushing $\left(t_{FT}/t_{FL}\right)$. Therefore, to maintain a given target overall product water recovery (Y_T) (i.e., to achieve a desired level of flushing as expressed by the target $F(\Theta)$ value), a longer filtration time would require a longer flushing time (t_{FL}) This would increase the maximum RO concentrate salt concentration ($c_{c,\max,n}$ per Equation 6) in each cycle, which increases osmotic pressure and energy consumption.

2.5. Range and Time for Average RO Concentrate Salt Concentrations

The ratio t_{FT}/t_{FL} establishes the overall product water recovery (Y_T per Equation 10, for a given Y_m). Accordingly, examination of Equations 6 and 8 indicates that the minimum and maximum RO concentrate salt concentration in each cycle of CRO operations depend on the overall water recovery. Also, these concentrations are expected to evolve with time (Figure 4) to extents that depend on the effectiveness of flushing—and thus the extent of inter-cycle salt accumulation. For high rejection membranes, with the reasonable approximation of complete salt rejection (R_{nom}=1), the minimum and maximum RO concentrate salt concentrations in CRO operations (e.g., Figure 4, for after any given n cycles, can be deduced by combining Equation 6, Equation 8, and Equation 10, yielding Equation 11 and Equation 12

Equation 11:

$$c^*_{c,\max,n} \equiv \frac{c_{c,\max,n}}{c_o} = \left(\frac{Y_T - \delta \cdot Y_m}{1 - Y_T}\right)\frac{1-\left(1-F\left(\Theta\right)\right)^n}{F\left(\Theta\right)}\Theta + \frac{1}{\left(1-\delta \cdot Y_m\right)}$$

Equation 12:

$$c^*_{c,\min,n} \equiv \frac{c_{c,\min,n}}{c_o} = \left(\frac{Y_T - \delta \cdot Y_m}{1 - Y_T}\right)\frac{\left(1-F\left(\Theta\right)\right)\cdot\left(1-\left(1-F\left(\Theta\right)\right)^n\right)}{F\left(\Theta\right)}\Theta + \frac{1}{\left(1-\delta \cdot Y_m\right)}$$

At sufficiently large number of cycles, the above minimum and maximum concentrations converge to stable values, becoming time invariant as expressed by Equation 13 and Equation 14:

Equation 13:

$$c^*_{c,\max,\infty} = \left(\frac{Y_T - \delta \cdot Y_m}{1 - Y_T}\right)\frac{\Theta}{F\left(\Theta\right)} + \frac{1}{\left(1-\delta \cdot Y_m\right)}$$

Equation 14:

$$c^*_{c,\min,\infty} = \left(\frac{Y_T - \delta \cdot Y_m}{1 - Y_T}\right)\frac{\left(1-F\left(\Theta\right)\right)\cdot\Theta}{F\left(\Theta\right)} + \frac{1}{\left(1-\delta \cdot Y_m\right)}$$

Equation 13 indicates that the flushing characteristics of the system (as quantified by $F\left(\Theta\right)$) determine the maximum concentrate salt concentration. Under ideal

plug flow conditions in the RO module, $\Theta / F\left(\Theta\right) = 1$ and $c^*_{c,\max,\infty}$ is at the lowest value. Dispersion, however, increases the magnitude of $\Theta / F\left(\Theta\right) > 1$, thus elevating $c^*_{c,\max,\infty}$ above the value that would be attained for an ideal plug.

In CRO operation, filtration duration is expected to be much longer than that of flushing. Energy consumption during the filtration period depends on the time average RO concentrate osmotic pressure and thus solute concentration. Given the linear RO concentrate salt concentration-time profile during the filtration period (i.e., for the special cases of complete/constant salt rejection as per Equation 5), the time average RO concentrate salt concentration is simply the arithmetic average of the minimum and maximum RO concentrate salt concentrations as shown in Equation 15 :

Equation 15:

$$c^*_{c,\text{ave},\infty} = \frac{1}{2} \cdot \left(c^*_{c,\min,\infty} + c^*_{c,\max,\infty} \right)$$

Combining Equation 13 and Equation 15 yields Equation 16:

Equation 16:

$$c^*_{c,ave,\infty} = \left(\frac{Y_T - \delta \cdot Y_m}{1 - Y_T} \right) \frac{\Theta \cdot \left(2 - F\left(\Theta\right)\right)}{2 \cdot F\left(\Theta\right)} + \frac{1}{\left(1 - \delta \cdot Y_m\right)}$$

Note that when flushing is relatively fast relative to filtration, the concentrate salt concentration profile during flushing can also be approximated with a linear profile. In this case, the average concentration during flushing can thus be also approximated by the arithmetic average of the minimum and maximum as in Equations 15 and 16.

In principle, plug flow ($F\left(\Theta\right)$=1) is desirable for minimizing $c^*_{c,ave,\infty}$ and therefore osmotic pressure for a given set of Y_T and Y_m. However, given that axial dispersion is unavoidable in real systems, $F\left(\Theta\right)$ must be determined experimentally for specific RO systems and modules. As an illustration, the effect of various $F\left(\Theta\right)$ behaviors on the time average RO retentate salt concentration is summarized in Table 1 or observed in the laminar flow in tubular and rectangular channels**.**

Clearly, the time average RO concentrate salt concentrations for CRO operations, at a given overall cycle (Y_T) and module water recovery (Y_m), is highly dependent on specific RO module flushing characteristics as quantified by $F\left(\Theta\right)$ and Θ. In

principle, the term $\Theta \cdot \left(2 - F\left(\Theta\right)\right) / 2 \cdot F\left(\Theta\right)$ in Equation 16 controls the impact of flushing characteristics and duration on the average concentrate salt concentration. Under plug flow conditions, the above term reduces to ½ (Table 1). Under non-ideal conditions (in which axial dispersion is important), the term reduces to $\Theta / 2$ when the maximum flushing duration is used to operate at near complete flushing ($F\left(\Theta\right) \approx 1$). This indicates that $c^*_{c,ave,\infty}$ (the time average RO concentrate salt concentration) will increase considerably when a long flushing duration (Θ) is required for complete flushing due significant axial dispersion in the RO module. In such a case, shorter flushing duration and thus incomplete flushing may result in lower $c^*_{c,ave,\infty}$ relative to operation in which flushing is incomplete.

Table 1. Examples of step response function, $F\left(\Theta\right)$, for different flows (Levenspiel, 1996) and the corresponding average cycle retentate salt concentration in CRO.

	$F\left(\Theta\right)$	$c^*_{c,\text{ave},\infty}$
Plug-flow	1 , $\quad t \geq \tau$	$\frac{1}{\left(1-\delta \cdot Y_m\right)} + \frac{1}{2}\left(\frac{Y_T - \delta \cdot Y_m}{1 - Y_T}\right)$
Laminar flow in circular channel	$1 - \frac{1}{2\Theta}, \quad t \geq \frac{\tau}{2}$	$\frac{1}{\left(1-\delta \cdot Y_m\right)} + \frac{1}{2}\left(\frac{Y_T - \delta \cdot Y_m}{1 - Y_T}\right)\left(\frac{2\Theta+1}{2\Theta-1}\right)\Theta$
Laminar flow in between two parallel plates	$\left(1 - \frac{2}{3\Theta}\right)^{1/2}, \quad t \geq \frac{2}{3}$	$\frac{1}{\left(1-\delta \cdot Y_m\right)} + \ldots$ $\frac{}{2}\left(\frac{Y_T - \delta \cdot Y_m}{1 - Y_T}\right)\left(2\left(1 - \frac{2}{3\Theta}\right)^{-1/2} - 1\right)\Theta$

2.6. Theoretical Minimum Specific Energy Consumption

To assess the potential energy benefits of CRO relative to conventional RO, we considered the theoretical minimum specific energy consumption (SEC) of CRO at the limit of the crossflow thermodynamic restriction ('tr'). In this case, the required applied pressure for RO operation ($p_{f,tr}$) is equal to the osmotic pressure of the RO concentrate as calculated in Equation 17:

Equation 17:

$$\frac{p_{f,tr}}{\pi_o} = \frac{\pi_c}{\pi_o} = c_c^*$$

In Equation 17, the relationship between solute concentration and osmotic pressure can be reasonably considered to be linear. To quantify energy consumption, the placement of pressure generating and recovering unit operations in the RO system configuration must be defined. For this purpose, an ideal CRO system depicted in Figure 6 can be considered.

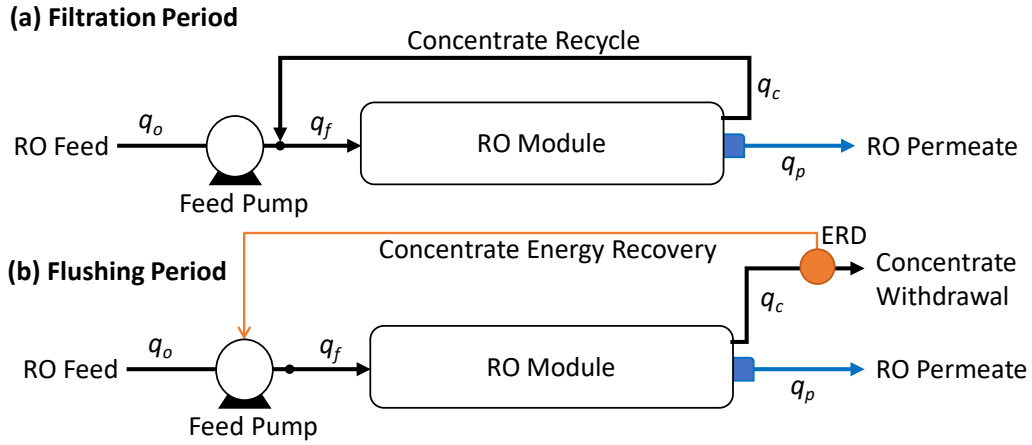

Figure 6. Cyclic RO system configurations during filtration and flushing periods.

In this ideal system, feed pumping is accomplished at the raw feed stream (the subscript 'o' modifying the q as a variable). In the concentrate recycle configuration during the filtration period, high pressure RO concentrate is directly recycled to the high-pressure RO feed stream (downstream of feed pump). Under the ideal condition, the axial pressure drop is assumed to be small. Therefore, one can consider a negligible energy footprint of a booster pump in the concentrate recycle stream which serves to enable recycling of the high pressure RO concentrate. Noting that $q_p = q_o$ (where CRO Feed = q_o) is kept at a target value during the filtration period, the instantaneous rate of work during the filtration period is given by Equation 18:

Equation 18:

$$W_{P,FT}(t) = \Delta p_f(t) \cdot q_o = \Delta p_f(t) \cdot q_p$$

where:

$W_{P,FT}$ is work during the filtration period

During the flushing period, the RO system is reconfigured to enable concentrate withdrawal. The raw feed flow rate (q_o) is increased to same level as the feed flow

rate (q_f) required to achieve the target RO module water recovery ($Y_m=q_p/q_f$) while maintaining water productivity at the target constant q_p. For the case of full recovery of the RO concentrate pressure energy (i.e., energy recovery device operating at an efficiency of η_{ER}=100 percent where η_{ER} is energy recovery device efficiency), the instantaneous rate of work during flushing is given by Equation 19:

Equation 19:

$$\dot{W}_{P,FL}(t) = \Delta p_f(t) \cdot \left(q_f - \eta_{ER} \cdot q_c\right) = \Delta p_f(t) \cdot q_p$$

Given the rate of work done during both the filtration and flushing periods, the SEC for CRO can be defined for a full cycle by Equation 20:

Equation 20:

$$SEC_{CRO} = \frac{\int_0^{t_{FT}+t_{FL}} \frac{\dot{W}_P(t)}{\eta_P} dt}{\int_0^{t_{FT}+t_{FL}} q_p \cdot dt} = \frac{1}{\eta_P} \cdot \frac{1}{(t_{FT}+t_{FL})} \int_0^{t_{FT}+t_{FL}} \Delta p_f \cdot dt$$

where:

η_P is the pump efficiency

Equation 20 is for the case of constant permeate production and, during flushing, complete concentrate energy recovery. Thus, Equation 20 indicates that, for 100 percent pump efficiency, the SEC is simply the time average transmembrane pressure over the entire cycle. At the limit of the cross-flow thermodynamic restriction (*tr*) and after a sufficient number of cycles to reach stable time average salinity of the RO concentrate (i.e., $c_{c,ave,\infty}$), substitution of Equation 16 into Equation 20 yields the relationship in Equation 21:

Equation 21:

$$NSEC_{CRO,tr,\infty} = c^*_{c,ave,\infty} = \left(\frac{Y_T - \delta \cdot Y_m}{1 - Y_T}\right) \cdot \frac{\Theta \cdot \left(2 - F(\Theta)\right)}{2 \cdot F(\Theta)} + \frac{1}{\left(1 - \delta \cdot Y_m\right)}$$

where:

CRO is SEC normalized with respect to the raw water osmotic pressure

which indicates that the CRO SEC normalized ($NSEC=SEC/\pi_0$) with respect to

the raw water osmotic pressure (π_0) is simply the average normalized time average concentrate salt concentration over the entire cycle. Equation 21 reveals that the SEC for CRO is a strong function of the flushing characteristics of the specific CRO system under consideration. It should be noted that the NSEC at the thermodynamic restriction limit is equivalent to the dimensionless time average RO concentrate salt concentration. Therefore, energy optimal operation should strive to minimize the time average RO concentrate salinity. Lastly, for comparing CRO to conventional RO, consider the NSEC of conventional steady-state RO, with concentrate energy recovery of efficiency of η_{ERD}, operated at the same overall water recovery (Y_T) as given below (Zhu et al. 2009) in Equation 22:

Equation 22:

$$NSEC_{SSRO,tr} = \frac{1-\eta_{ERD}\left(1-Y_T\right)}{Y_T\left(1-Y_T\right)}$$

2.7. Model-Based Process Control

We used the process models presented in the above discussion as the basis for developing a model-based process control for CRO operation. For such basic control, CRO operation requires determination of the filtration (t_{FT}) and flushing (t_{FT}) durations for a given RO module per-pass water recovery (Y_m) in order to achieve a given target overall water recovery (Y_T). For this purpose, a step response to a step input should ideally be characterized experimentally for the system under consideration. Such information would allow determination of the system flushing characteristics in terms of the $F\left(\Theta\right)$ as defined in Equation 7. As implied by Equation 21, the flushing characteristics govern the time average RO concentrate salinity and, therefore, directly impact the energy footprint of the RO system. For this purpose, the model in Equation 16 can be used determine the optimal flushing duration ($\Theta_{FL} = t_{FL} / \tau_{FL}$) that minimizes $c^*_{c,ave,\infty}$. Given the optimal Θ_{FL}, the following equation, obtained by rearrangement of Equation 10, can be used to determine the required filtration time for given a target overall cycle water recovery (Y_T) in Equation 23:

Equation 23:

$$t_{FT} = \left(\frac{Y_T - \delta \cdot Y_m}{Y_m \cdot \left(1-Y_T\right)}\right) \cdot \tau_{FL} \cdot \Theta_{FL}$$

Cyclic RO must be operated at or below the overall water recovery limit ($Y_{T,hi}$).

This limit can be governed by membrane scaling/fouling, as well as by system pressure rating. The process models developed in previous sections can be used to estimate the feasible overall water recovery range as Equation 24:

Equation 24:

$$Y_m < Y_T < Y_{T,hi}$$

where:

$Y_{T,hi}$ is the water recovery in which a maximum allowable high limit of RO concentrate salt concentration ($c_{c,hi}$) is reached.

The value of $c_{c,hi}$ (the maximum allowable high limit of RO concentrate salt concentration) can be dictated, for example, based on the maximum allowable osmotic pressure (and thus the maximum allowable applied pressure to achieve the target permeate flux) or the maximum concentrate salt concentration to minimize membrane mineral scaling. The relationship between $Y_{T,hi}$ and $c_{c,hi}$ can be determined by rearranging Equation 16 to yield Equation 25.

Equation 25:

$$Y_{T,hi} = \frac{\delta \cdot Y_m \cdot \frac{\Theta_{FL}}{F\left(\Theta_{FL}\right)} + \frac{c_{c,hi}}{c_o} - \left(1 - \delta \cdot Y_m\right)^{-1}}{\frac{\Theta_{FL}}{F\left(\Theta_{FL}\right)} + \frac{c_{c,hi}}{c_o} - \left(1 - \delta \cdot Y_m\right)^{-1}}$$

Therefore, given a limit on $c_{c,hi}$, the maximum overall water recovery for a given RO system can be estimated in real time based on sensor data of raw feed water concentration (c_o). This should allow determination of the appropriate filtration (t_{FT}) and flushing (t_{FT}) durations for effective and energy efficient CRO operation via an embedded model-based controller. The overall strategy for the control approach is summarized in Figure 7,

where:

$Y_{T,\,user}$ is the overall product water recovery defined by the suer

$Y_{T,\,target}$ is the overall target product water recovery

$C_{cMax,\,\infty}$ is the RO concentrate salt concentrations in CRO operations for high number of flux cycles.

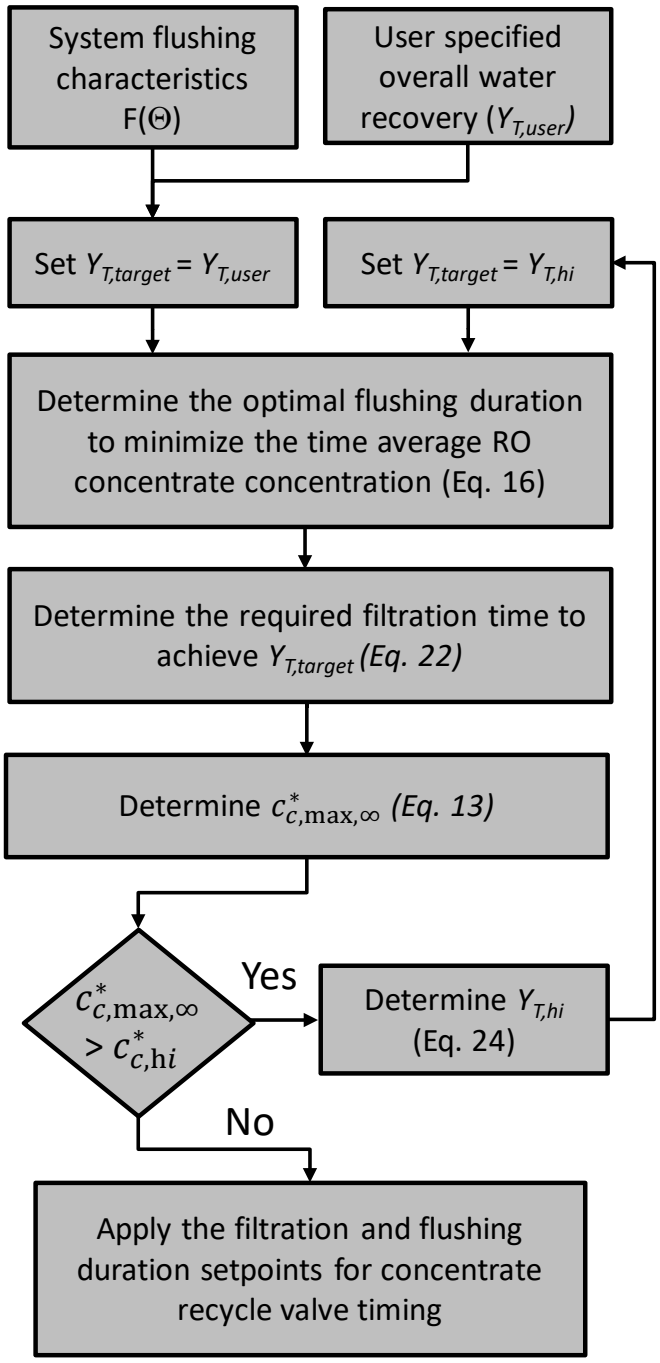

Figure 7. Process control strategy for optimal CRO operation.

3. Experimental Description

3.1. Cyclic RO System Development

A CRO system was developed by retrofitting an existing RO system (Newport 400 MK II, Spectra Watermakers, San Rafael, CA). The system (Figure 8 and Figure 9) contained a single 2.5 x 40 inch RO element (Dow Filmtech SW30-2540) for fresh water production up to 380 gallons per day (GPD).

- ***Raw feed.*** Raw feed water, pre-treated with filter cartridges (5 μm cellulose pleated 2-$^{1}/_{2}$ x10 inch, 20 micrometer (μm) pleated 2-1/2x10, Ocean Link Inc., Portsmouth, Rhode Island), was mixed with the concentrate-recycle from the membrane module using a low pressure booster pump (Model DRIVE D5 Strong, Laing Pumps, Medford, Oregon).

- ***Feed stream.*** The pressure of the feed stream was then increased using a specialized pumping system which operates with 24V DC voltage. The feed stream, whose volumetric flow rate was controlled using the pump's DC speed controller (Model NEMA 4X, DART Controls, Zionsville, Indiana), was fed to the membrane module.

- ***Recovery.*** The per–pass RO module water recovery was fixed in the system at 10 percent.

- ***Monitoring.*** Flow transmitters (Signet 8550, George Fischer Signet, Inc. El Monte, California) were installed for the feed and the permeate streams so that the product water recovery could be easily measured. Conductivity measurements of the raw-feed, feed, concentrate and the permeate stream were obtained using conductivity transmitters (Signet 2850, George Fischer Signet, Inc. El Monte, California) to monitor the variation in salinity during cyclic operation. The pressures of the feed, permeate, and the retentate streams of the CRO were monitored using in-line pressure transducers (Type S-20 4-20 mA, Wika, Klingenberg, Germany). An embedded Process Automation Controller (PAC) was installed to enable real time data acquisition of sensor measurements and automated process control of the system actuators.

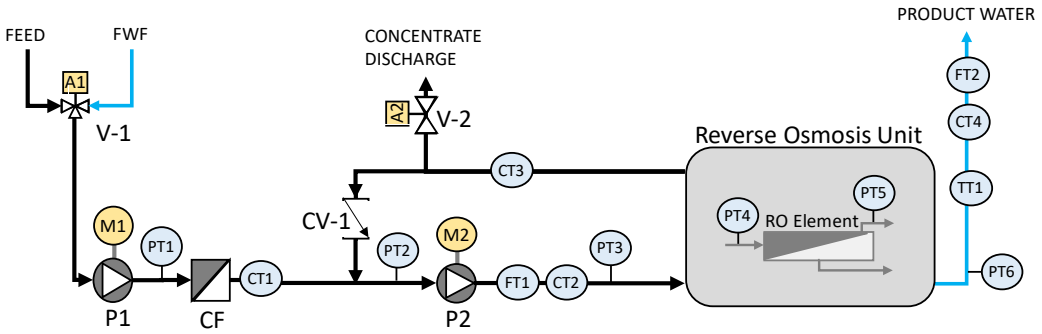

Figure 8. Process control strategy for optimal CRO operation.

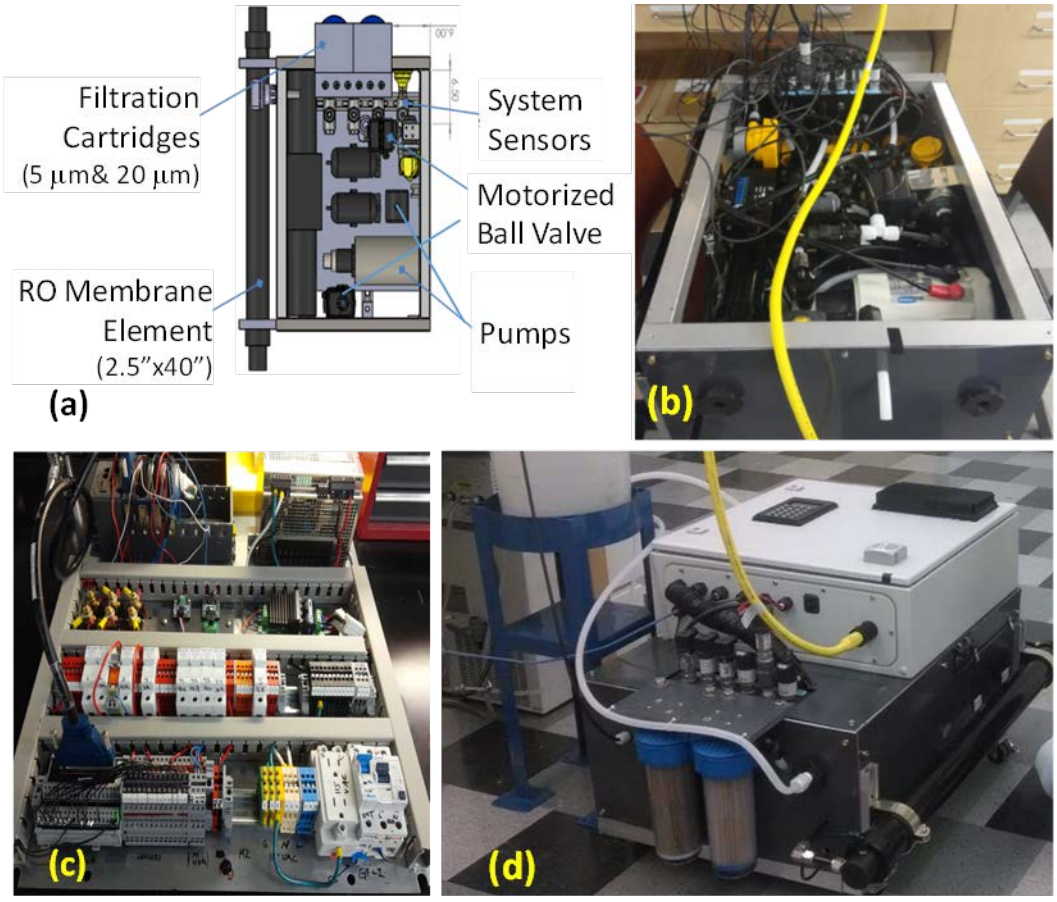

Figure 9. Photographs of the UCLA CRO system: (a) physical design, (b) body construction, (c) electrical circuit box, and (d) assembeled CRO system.

3.2. Implementation of Cyclic RO Process Control

A model-based controller was developed for the CRO system based on the control architecture depicted in Figure 10.

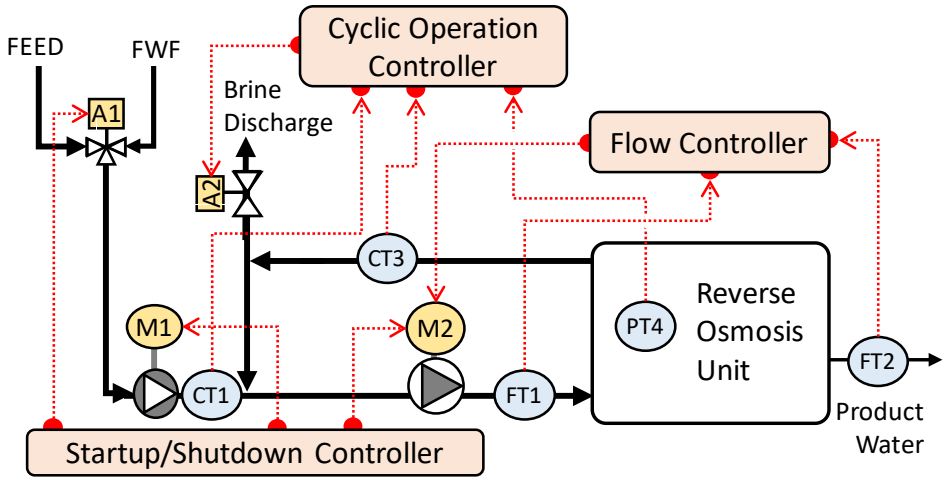

Figure 10. Process control strategy for optimal CRO operation.

Briefly, a startup-shutdown controller was implemented to enable sequence startup/shutdown of the feed booster pump motor (M1) and main pump motor (M2). A proportional-integral (PI) controller enabled control of the main pump motor (M2) to maintain either the RO unit feed flow rate (FT1) or product flow rate (FT2) at the relevant setpoint values. Note that in the present prototype RO unit, the per-pass module RO water recovery (Y_m) was mechanically fixed at about ten percent as this is a small test system. For cyclic operation, however, the extent of concentrate recycle governed the recovery. The flow rates were measured in FT2 and FT1 and are always at a ratio equivalent to Y_m. Finally, based on the approach depicted in Section 2.7. *Model-Based Process Control*, the cyclic model-based control approach was implemented for estimating the:

a. Feasible range of water recovery based on real-time raw water concentration

b. Appropriate filtration and flushing durations based on the overall water recovery set point, which is the higher of the user setpoint or the highest feasible level allowed by the system ($Y_{T,hi}$ per Equation 27)

The cyclic operation controller was also set to monitor the RO concentrate's salt concentration and the RO unit pressure to ensure that the above parameters ido not exceed the system physical constraints.

Finally, we developed a graphical user interface (Figure 11) to access the various controllers and specify system setpoints such as the target water recovery ($Y_{T,Target}$) and the desired level of flushing effectiveness (Φ).

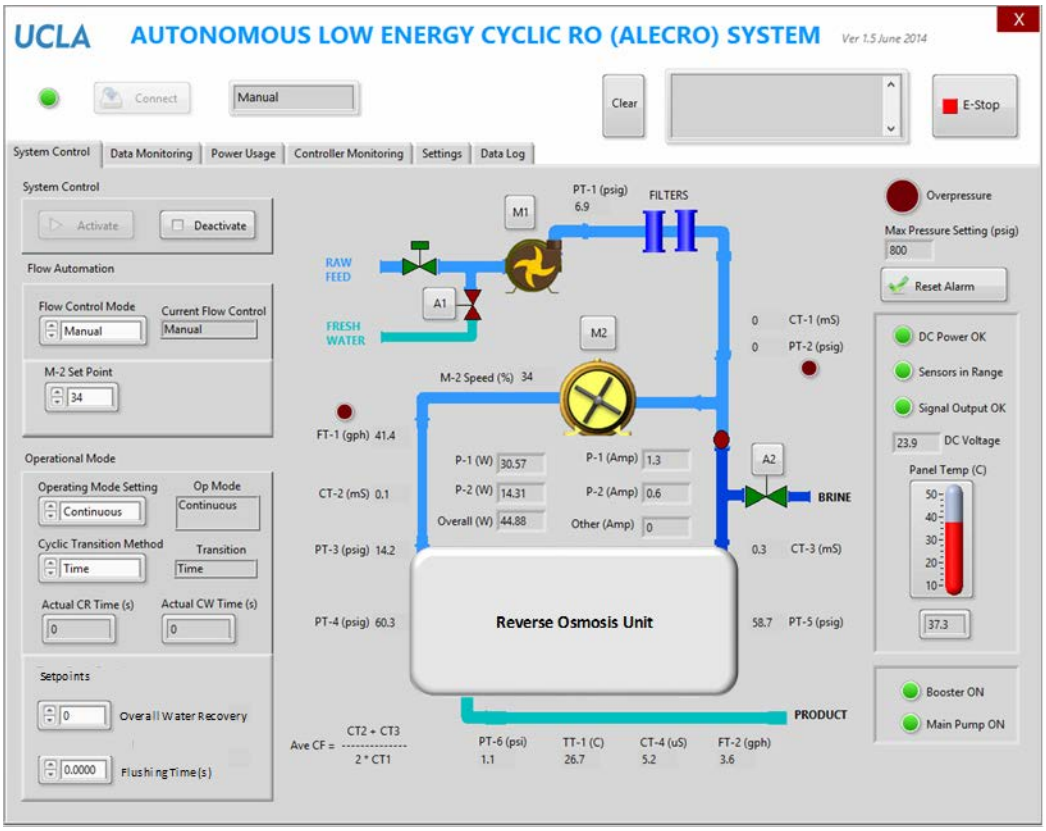

Figure 11. Process control strategy for optimal CRO operation.

3.3. Cyclic RO System Operation

Experimental evaluation of the CRO system was conducted both in the laboratory and in the field. As shown in Figure 12, feed water was supplied to the CRO system from a 200 liter (L) feed water tank. The concentrate and product water from the CRO system was recycled to the feed water tank. In the cyclic system operation's filtration period, the brine-discharge valve was completely closed to allow the concentrate stream to continuously mix with the raw feed water. In this period, the RO system operated in "closed-circuit" mode, desalting raw feed input into the product water at 100 percent water recovery. At the end of the filtration period, the brine discharge valve was opened to discharge the concentrated brine stream from the system. Only the fresh raw feed water was introduced to the membrane module to reduce the feed water salinity in the membrane in the flushing period. In the CRO experiment, the RO system was operated in a cyclic manner: alternating between filtration and flushing modes but continuously producing permeate water. To maintain the optimal performance of the hydraulic components, feed water flow rate was maintained constant at 2.83 gallons per minute (GPM) both in filtration and flushing period, corresponding to 380 GPD of constant permeate water production.

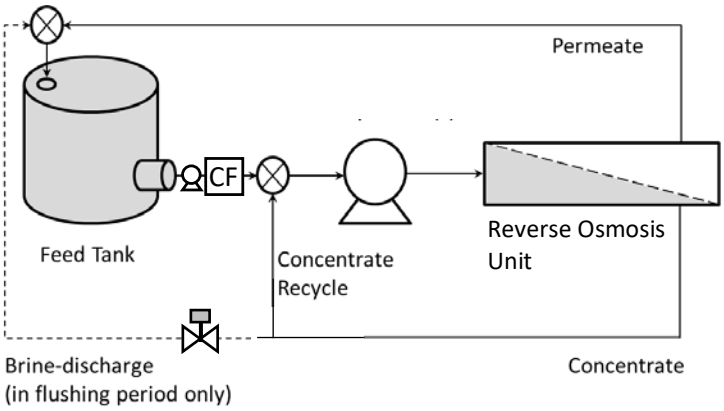

Figure 12. Experimental setup of the UCLA CRO system.

The CRO system was also field deployed in the Seawater Desalination Test Facility at the Naval Base Ventura County (NBVC) in Port Hueneme, California (Figure 13). An existing ultrafiltration (UF) unit at the above facility provided feed water for the CRO feed water tank. To test CRO desalting at various levels of feed salinity, batches of feed water with varying salinity were prepared by diluting ultra-filtered seawater to various extents with the available permeate water. The system was operated over the feasible range of water recovery for each level of feed water salinity.

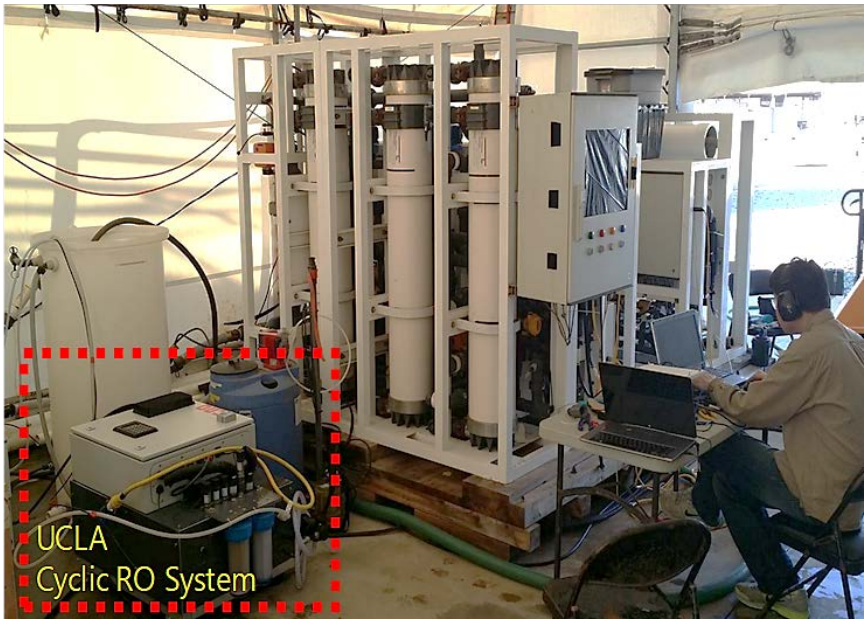

Figure 13. Deployment of the UCLA CRO system at the Naval Facilities Engineering Command's Seawater Desalination Test Facility (NAVFAC SDTF) in Naval Base Ventura County.

3.4. Determination of CRO System Flushing Characteristics

As discussed in Section 2. *Cyclic Process Modeling and Analysis*, the RO system's flushing characteristics is critical in CRO operational performance. Therefore, we conducted experiments to determine the decrease in RO concentrate salt concentration in response to a negative step input of RO feed concentration. The cumulative distribution of CRO concentrate salt concentration in response to a step decrease in RO feed concentration (at Θ=0) is given in Figure 14 in terms of the F(Θ) (i.e., the fraction of solute mass that is discharged out of RO system during the flushing period) as defined in Equation 7. A time delay up to Θ_o was observed until the first change in RO concentrate salt concentration is observed with a step change in RO feed salinity.

An empirical cumulative distribution function (Equation 26) was fitted to the data shown in Figure 15 for the present CRO system:

Equation 26:

$$F(\Theta)=\begin{cases}0, & \text{for } \Theta \le \Theta_o \\ 1-\exp\left(-\left(\dfrac{\Theta-\Theta_o}{\beta}\right)^{\frac{1}{\alpha}}\right), & \text{for } \Theta > \Theta_o\end{cases} \qquad (25)$$

where the fitted parameter values are Θ_o= 0.66, α=1.3, and β=0.987.

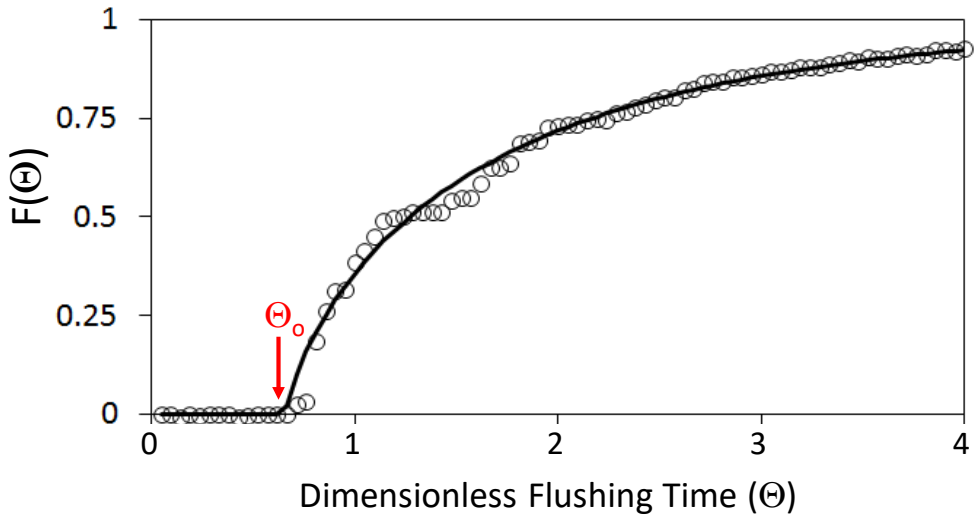

Figure 14. Experimental data of the distribution function, F(Θ), for the UCLA CRO system (Figure 9) flushing characteristics. The solid curve represents the empirical model fit (Equation 26) for the data obtained for the UCLA CRO system, where $\Theta = t/\tau_{FL}$ and τ_{FL} = 21.6 seconds.

4. Results and Discussion

4.1. CRO Operation in the Laboratory Testing

The capabilities of the small RO system developed in the present study (Figure 9) for CRO operations were evaluated experimentally over a range of operating conditions. Specifically, the system was operated with alternating modes of concentrate recycle (CR) and concentrate withdrawal (CW), leading to alternating periods of filtration (FT) and flushing (FL). The example shown in Figure 15 and Figure 16 illustrates the common time evolution of flow rates and salt concentrations in the system. In this example, the source water was diluted ultrafiltered seawater, the raw feed water salinity was 2,000 milligrams per liter (mg/L), and the overall water recovery rate was 44 percent. During CR mode, raw RO feed, RO feed, and RO permeate flow rates are maintained at constant values (Figure 15) that correspond to a fixed RO module per pass water recovery (about ten percent) to achieve the target water productivity of 1 liter per minute (L/min). Because the entire RO concentrate was recycled, salt slowly accumulates in the RO retentate stream, leading to increasing RO concentrate salt concentration and thus requiring proportional increases of the RO applied pressure (Figure 16) to maintain constant RO permeate production.

Upon reaching a prescribed (or threshold) salt concentration limit, the CR mode can be switched to CW to begin the flushing period. The flushing period is characterized by a step increase in the raw feed flow rate while water productivity and RO module per-pass recovery are kept fixed (Figure 15). Because RO concentrate is not recycled, flushing leads to reductions in RO retentate salt concentration and thus lowering the required applied RO feed pressure. However, due to concentration-driven salt transport across the membrane, the RO permeate concentration also varies with time, paralleling the transient profile of the RO retentate concentration (Figure 16). Despite these variations, membrane salt rejection (and thus permeate salt concentration) remains within acceptable ranges (see Figure 16). The data in Figure 15 and Figure 16 illustrates the capabilities of the present laboratory system for short-term cyclic operation. The capability for longer-term multi-cycle operation is discussed in Section. 4.2. *Cyclic RO Operation over Multiple Cycles.*

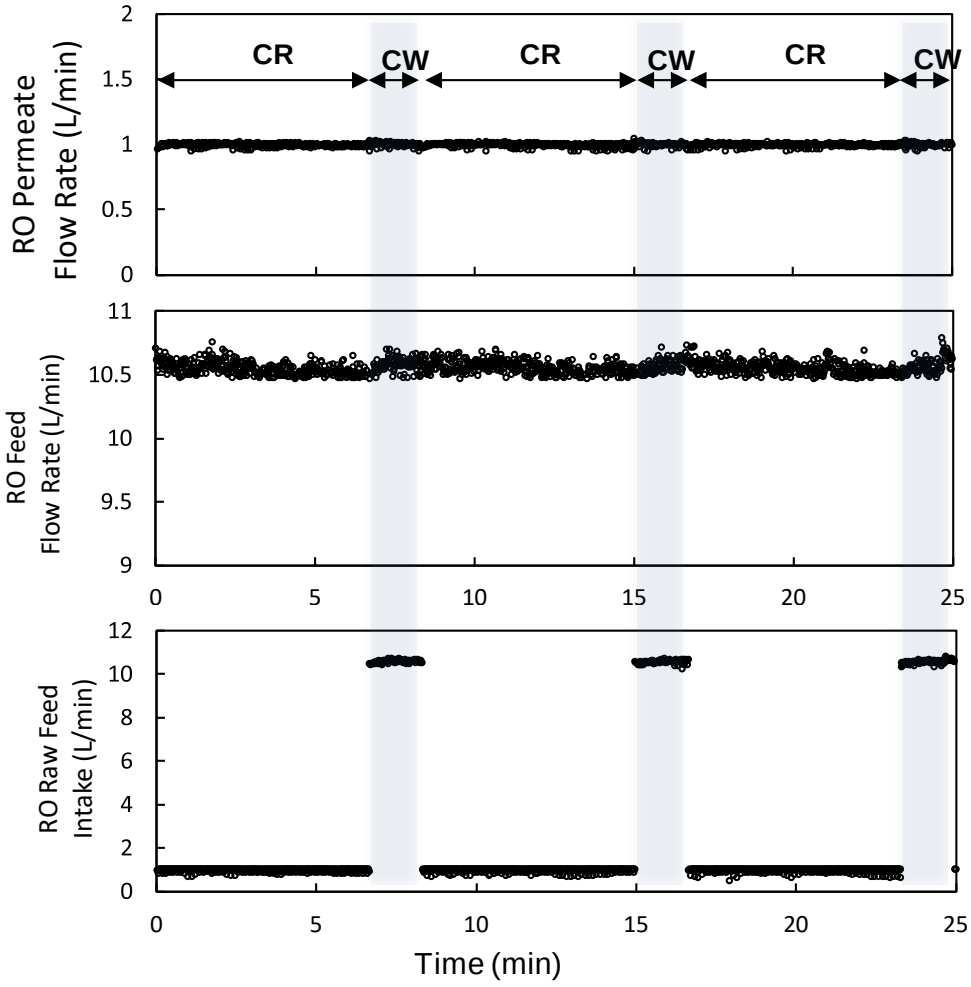

Figure 14. RO permeate, RO feed, and RO raw feed flow rates for the UCLA CRO system example (raw feed water salinity: 2,000 mg/L; overall water recovery: 44%).

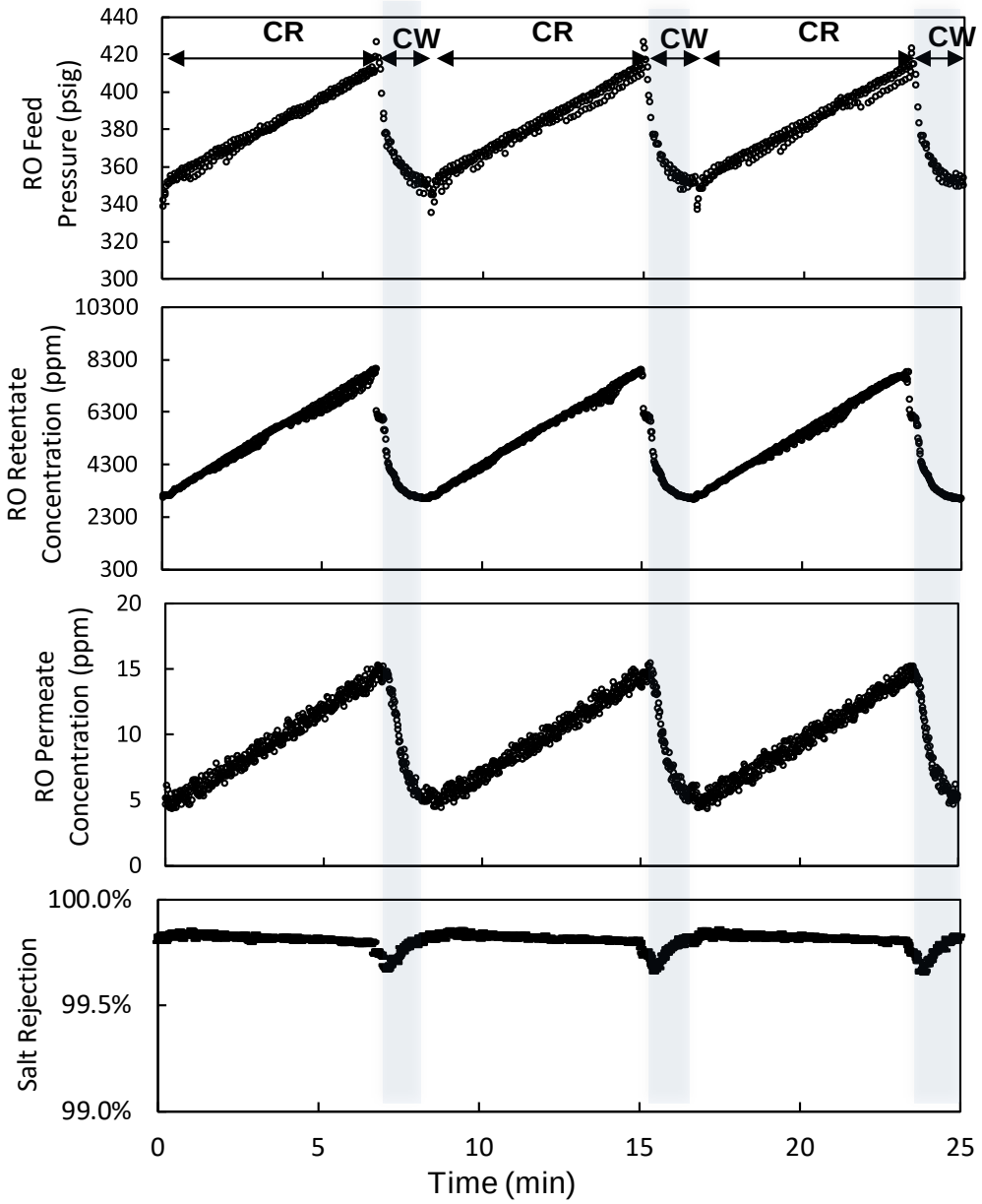

Figure 15. RO feed, retentate, and permeate salt concentrations in CRO operation. example (diluted ultrafiltered seawater, raw feed water salinity: 2,000 mg/L, and overall water recovery: 44%).

4.2. Cyclic RO Operation over Multiple Cycles

In multi-cycle operations, inter-cycle salt accumulation in the RO retentate stream, in addition to intra-cycle salt accumulation, can have significant impact on the range of RO concentrate salt concentration levels of each cycle ($c_{c,min,n} \leq c_{c,,n} \leq c_{c,max,n}$) and for extended system operation ($c_{c,min,\infty} \leq c_{c,\infty} \leq c_{c,max,\infty}$; see Figure 3). As can be deduced from Equation 11: through Equation 14:, the range of the concentrate salt concentration levels during cyclic operation depends not

only on the per-pass RO module water recovery (Y_m) and the target overall system water recovery (Y_T), but more importantly on the system's flushing characteristics as quantified by $F(\Theta)$.

To evaluate the impact of system's flushing characteristics on the RO process performance, experiments were conducted, comparing operation at the same Y_T of 50 percent and Y_m of 10 percent were conducted at short (25-second) and long (100-second) flushing durations, corresponding to $F(\Theta)$ values of 55 percent and 95 percent. As shown by the experimental data in Figure 17a and Figure 18a, a short flushing duration requires a short filtration duration as governed by the target overall water recovery (Y_T) per Equation 10. Since flushing was incomplete ($F(\Theta)$=55%), the run was characterized by inter-cycle salt accumulation as indicated by increasing $c_{c,min,n}$ values up until a stable $c_{c,min,\infty}$ was reached after more than 10 cycles. In contrast, longer flushing durations (Figure 17b and Figure 18b) in turn required longer filtration durations and thus a higher extent of intra-cycle accumulation to maintain the same target system water recovery (Y_T) per Equation 10. When flushing is near completion ($F(\Theta)$=1), there is negligible inter-cycle salt accumulation and thus $c_{c,min,n} \approx c_{c,min,,\infty}$ is close to the steady-state value ($c_{c,ss}$) at the per pass module water recovery (Y_m=10%). Indeed, comparison of $c_{c,max,\infty}$ between the two runs (Figure 18) indicates that complete flushing leads to higher $c_{c,max,\infty}$ due to the longer required l flushing time and thus filtration duration (i.e., to maintain the same Y_T). These are consistent with predictions derived from Equation 11 through Equation 14 with regards to the minimum and maximum concentrate salt concentrations (Figure 18).

The experimental run at a short 25-second flushing (Figure 18a and Figure 18b) can be further examined by comparing the run's results with the CRO model developed in Section 2. *Cyclic Process Modeling and Analysis* to predict both inter- and intra-cycle salt accumulation in the RO retentate stream (Figure 19 and Figure 20). Intra-cycle salt accumulation occurred during the filtration period, and the model predicted a linear increase in RO concentrate salt concentration with time in this filtration period as per Equation 6. UsingEquation 12 to predict $c_{c,min,n}$ in Equation 6 for each cycle allows for the determination of the RO concentrate salt concentration profile in multiple cycles and thus the effect of inter-cycle salt accumulation due to incomplete flushing. In the case of CRO at 50 percent overall water recovery with 25-second flushing ($F(\Theta)$=55 percent), incomplete flushing led to inter-cycle salt accumulation that was characterized by increasing $c_{c,min,n}$ and $c_{c,max,n}$ until the corresponding stable values were reached (Figure 20). Indeed, as shown in Figure 19 and Figure 20, the theoretical predictions fit well to the experimental data.

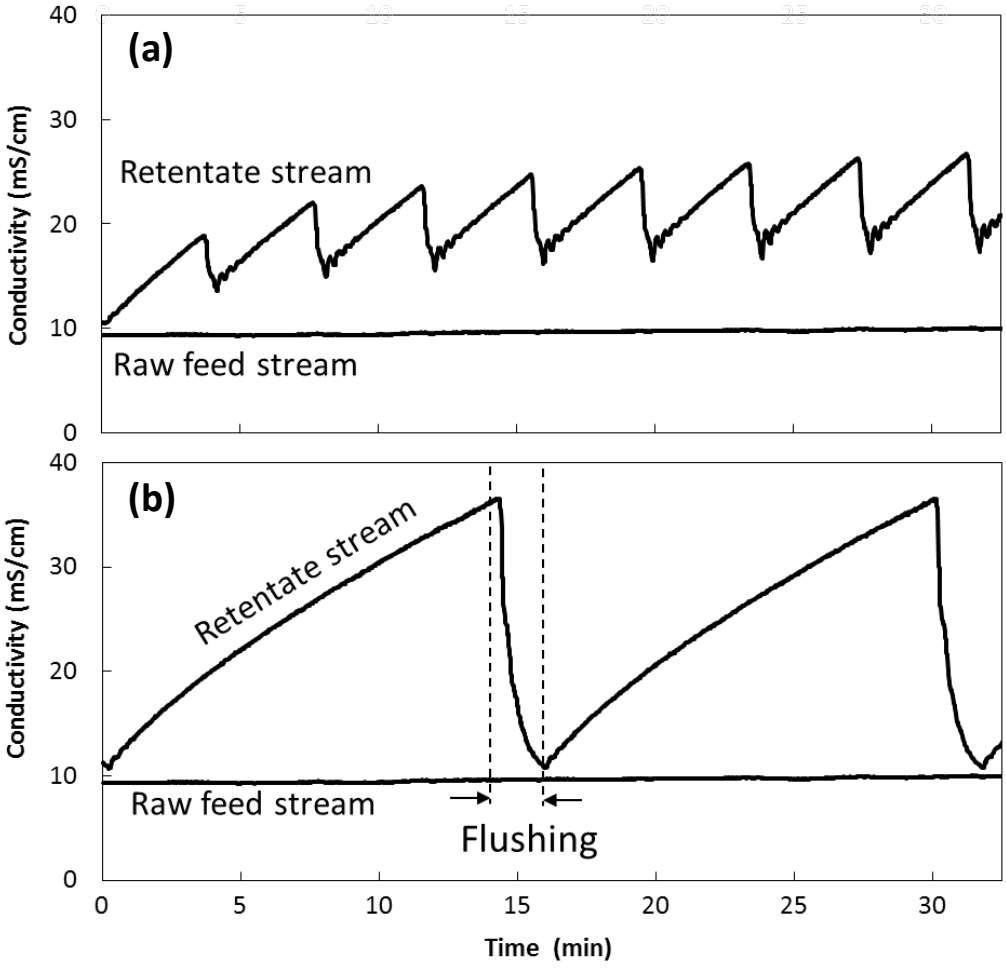

Figure 16. Profiles of the retentate concentration (measured at the membrane element exit) and the raw-feed streams during CRO operation for 50 percent overall product water recovery at a constant permeate flux of 14.0 gallons per square foot per day (GFD) for (a) F(Θ)=55% (25 seconds flushing period), and (b) F(Θ)=95% (100 seconds flushing period).

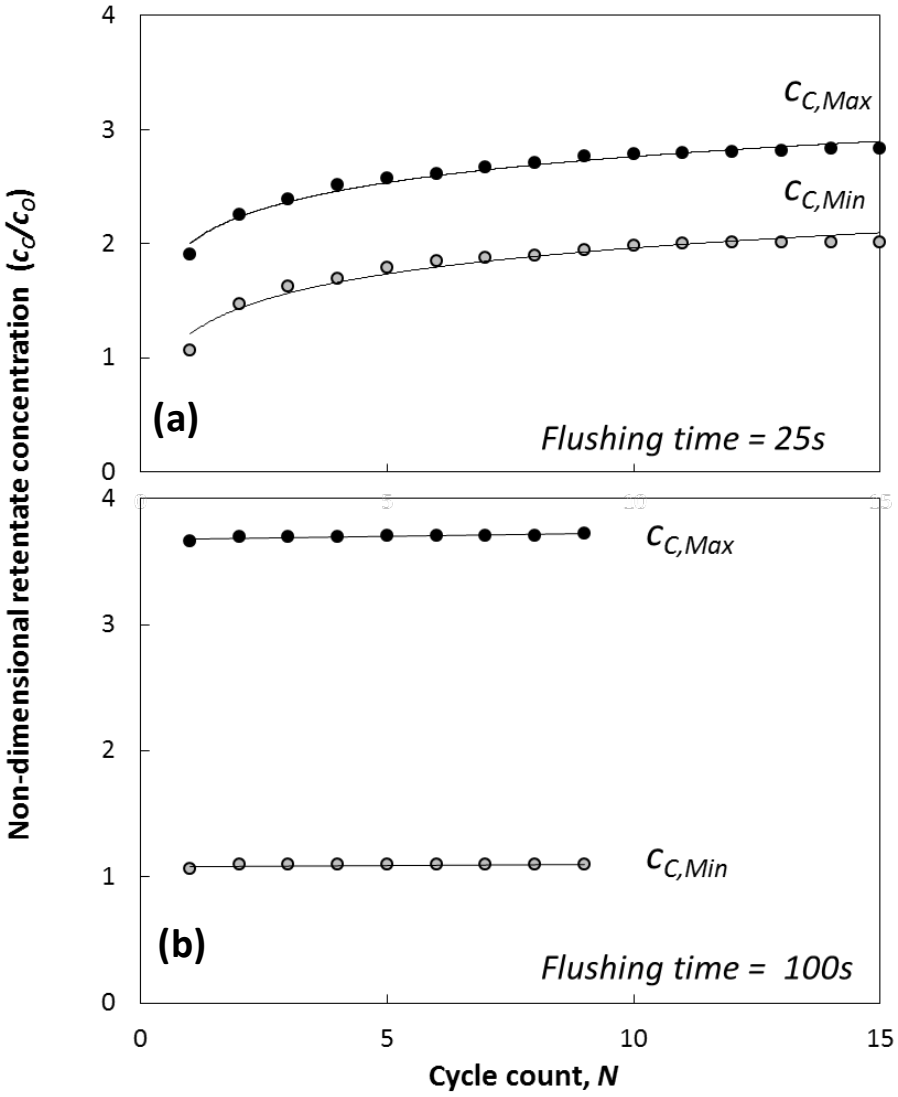

Figure 17. Profiles of the retentate concentration (measured at the membrane element exit) and the raw-feed streams during CRO operation at 50% overall product water recovery and constant permeate flux of 14.0 GFD for (a) F(Θ)=55%, and (b) F(Θ)=95%.

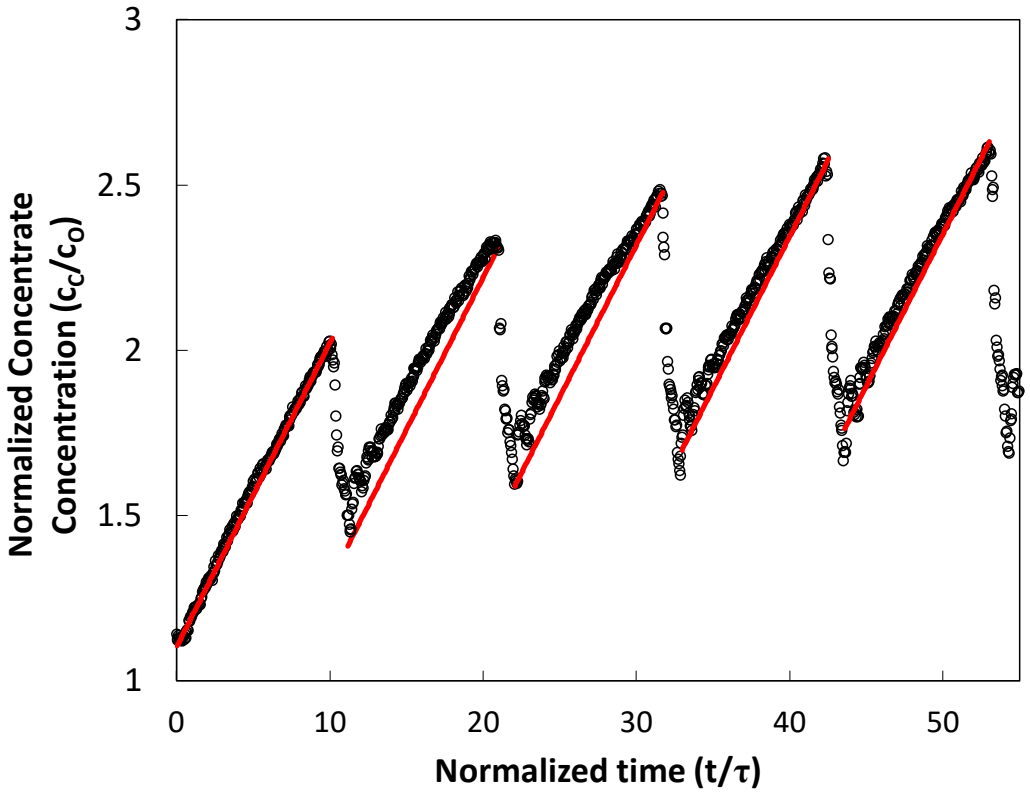

Figure 18. Measured and predicted normalized concentrate salt concentraion profiles during CRO operation at overall water recovery of 50% at a constant permeate flux of 14.0 GFD for F(Θ)=55% (25-second flushing period).

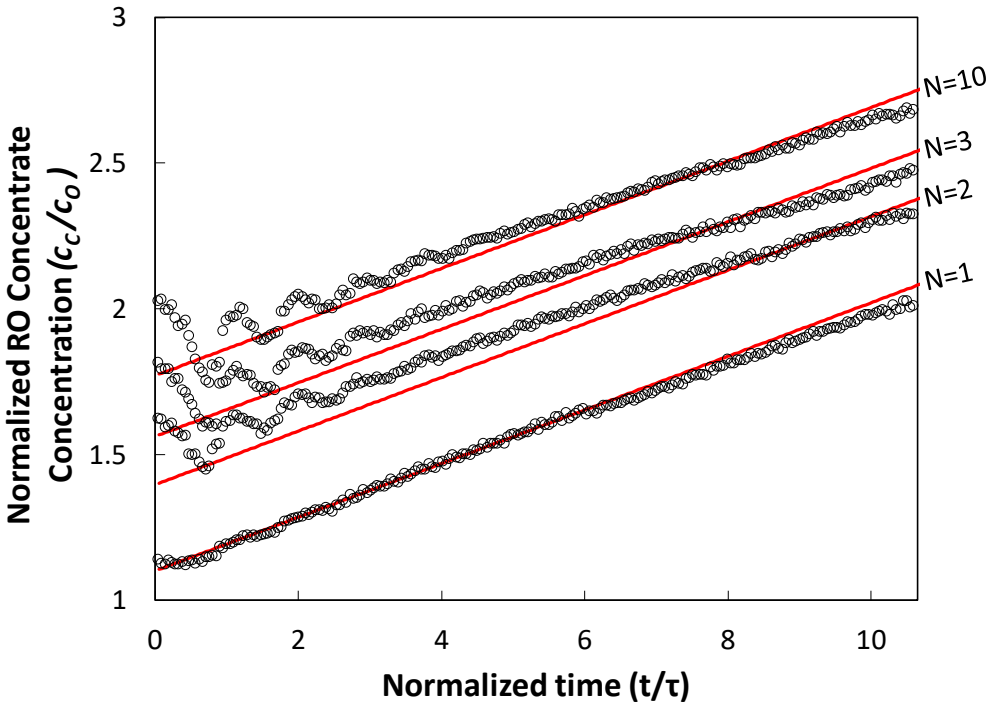

Figure 19. Measured and predicted normalized concentrate salt concentration profiles during filtration periods of CRO operation at overall water recovery of 50 percent for a constant permeate flux of 14.0 GFD and F(Θ)=55% (25-second flushing).

For CRO operation at a given set of target overall water reocovery (Y_T) and specific system's per pass RO module recovery (Y_m), the stable maximum (Equation 13), minimum (Equation 14)—and therefore the time-average (Equation 16)—RO concentrate salt concentration are highly dependent on the specific RO system's flushing characteristics ($F(\Theta)$) and thus the applied flushing duration. To further explore the interplay of the above parameters, flushing duration (Θ, corresponding to a specific $F(\Theta)$ value) and overall water recovery (Y_T) was systematically varied in a set of CRO experiments (Table 2) in which the $F(\Theta)$ values were determined based on the empirical fit of Equation 26 to the experimental data. As shown in Figure 21, higher extents of flushing (as characterized by a value of $F(\Theta)$ approaching unity) lead to increasingly high time-average RO concentrate salt concentration for a given Y_T and, as expected, with increasing Y_T. The results are non-intuitive as short flushing durations, characterized by low values of $F(\Theta)$ (Table 2) appear to lead to lower time average RO salt concentrations despite having higher degrees of inter-cycle salt accumulation. Complete flushing, which practically eliminates inter-cycle salt accumulation, leads to higher time-average RO concentrate salt concentration. This suggests that in CRO, intra-cycle salt accumulation has a much greater impact on the time average RO concentrate salt concentration than on inter-cycle

salt accumulation. The data appears to indicate that a flushing duration corresponding to an $F(\Theta)$ value of about 40-50 percent was sufficiently short to balance the impacts of both intra- and inter-cycle salt accumulation on the time average RO concentrate salt concentration. As indicated in Section 2.5. *Range and Time for Average RO Concentrate Salt Concentrations*, the time average RO concentration has a direct impact on CRO energy consumption, which is discussed in the Section 4.3. CRO *Energy Consumption*.

Table 2. Cyclic RO experimental matrix of test conditions

Test #	Flushing Time (seconds)	Filtration Time (seconds)	Overall Water Recovery (Y_T)
1	8	60 119 213 280	46.4 61.6 73.7 78.5
2	25	189 370 665 875	46.4 61.6 73.7 78.5
3	40	302 592 1,065 1,400	46.4 61.6 73.7 78.5
4	50	375 745 1,330 1,750	46.4 61.6 73.7 78.5
5	100	755 1,480 2,660 3,500	46.4 61.6 73.7 78.5

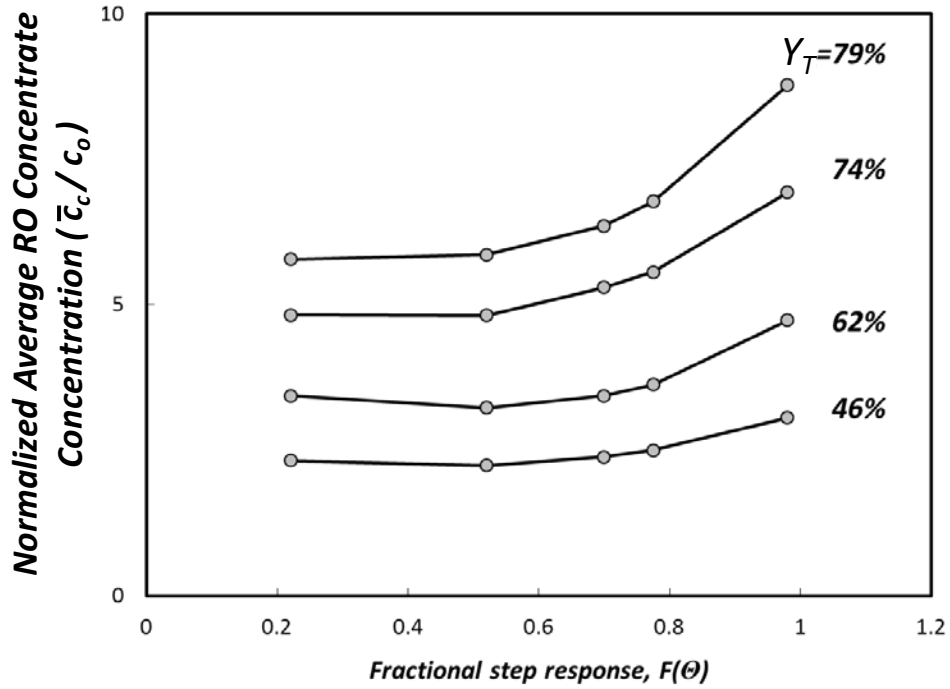

Figure 21. Variations of the normalized average RO concentrate salt concentration ($\bar{c}_c / c_o$, where $\bar{c}_c \approx (c_{c,\max} + c_{c,\min})/2$) with the extents of flushing as quantified by the fractional step response function F(Θ) (for flushing duration in the range of 60-3,500 seconds; see Table 6.1) for various overall product water recovery levels (YT).

4.3. CRO Energy Consumption

The potential energy benefits of CRO was evaluated on the basis of the theoretical normalized specific energy consumption (NSEC; Equation 21) relative to steady state RO (SSRO; Equation 22) with (η_{ERD}=100%) and without (η_{ERD}=0) an energy recovery device, comparing all at the same overall water recovery (Y_T) for operation at the limit of the crossflow thermodynamic restriction. To incorporate the impact of RO system flushing characteristics on the NSEC, specific cases of ideal plug flow, laminar flow in a circular pipe, and laminar flow in thin rectangular membrane channels were considered based on the relations presented in Table 1, as well as per the flushing characteristic of the present laboratory system (Equation 26). In both long (Θ=4; Figure 22a) and short (Θ=1**;** Figure 22b) flushing durations, CRO can achieve lower NSEC than steady state RO with energy recovery device only when ideal plug flow condition can be attained during flushing of the RO retentate channel. In practice, however, axial dispersion will occur in the RO retentate channel during flushing. Thus, under more practical flow conditions (e.g., laminar flow in a circular tube, thin rectangular channel, or the current laboratory experimental system containing spiral-wound element with spacers), CRO cannot perform better than SSRO equipped with an ERD for both long (Figure 22a) and short flushing durations (Figure 22b).

The RO system was operated at permeate flux of 14.0 gallon/ft^2-day with a raw feed water solution salinity of 1,000 mg/L NaCl. Steady-state RO (SSRO) operated at recovery YT; ERD: energy recovery device. Note that at the same total recovery, Y_T, a given CRO system that operates at a shorter flushing period (Figure 22b) would result in lower NSEC relative to operation at a longer flushing period (Figure 22a). At the lower recovery range, the NSEC for CRO can be lower than for a steady state reverse osmosis (SSRO) that operates without an ERD, but is higher at the high water recovery range. However, it is emphasized, solute dispersion during flushing does lead to a higher NSEC for the cyclic process than for SSRO with an ERD.

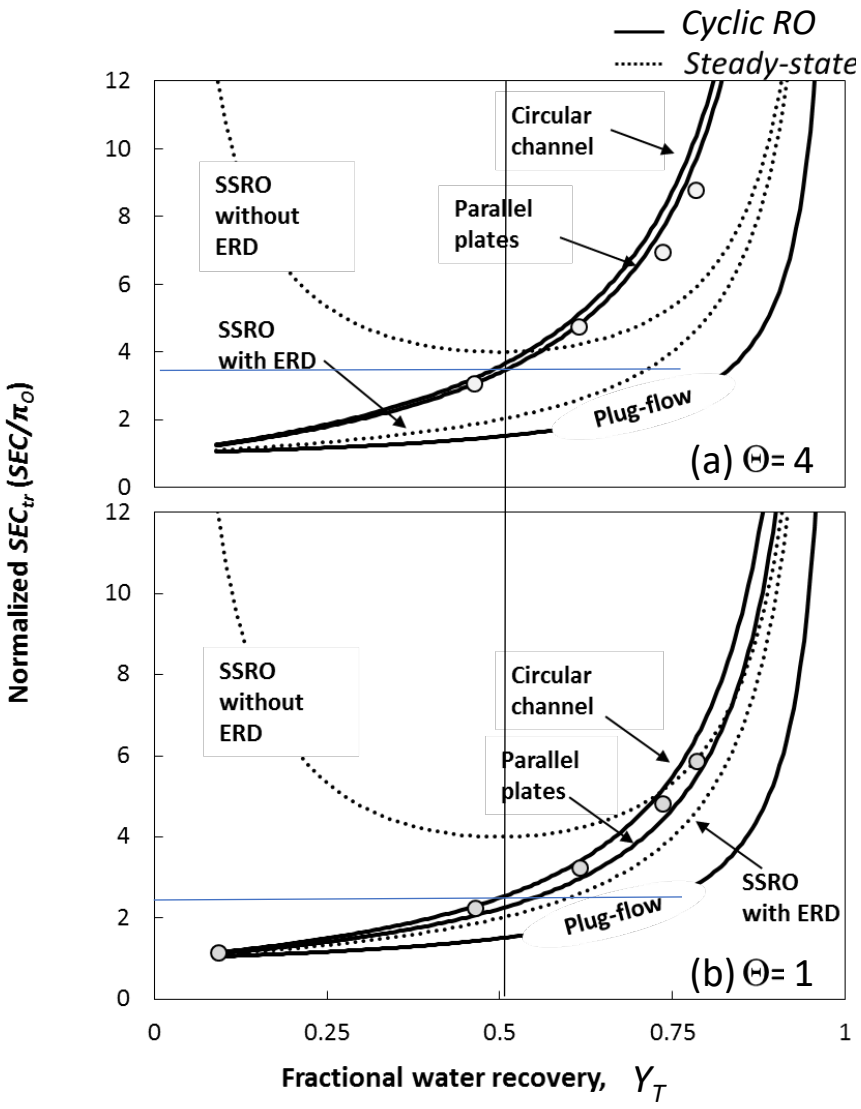

Figure 22. Variation of the normalized SEC with fractional product water recovery for flushing time, Θ (=tFL/τ) of 1 (a) and 4 (b).

CRO Field Demonstration

A key advantage of CRO is the ability to operate over a wide range of water recovery with a single system platform. The recovery range, however, is governed by the feed water salinity and its osmotic pressure relative to that which can be accommodated by the system's maximum operational pressure limit. To enable autonomous operation, CRO control systems need to be able to predict the practical water recovery range for a given feed water condition and subsequently establish energy-optimal operation. To this end, UCLA conducted a field to evaluate the effectiveness of a model based controller as per Section 2.7. *Model-Based Process Control* for guiding the RO system operation for different levels of feed water salinity. As shown in Figure 23, the maximum system pressure limit was increased rapidly with rising feed water salinity. As a consequence, the cycle duration was much shorter and cycle frequency higher at higher feed water salinity. For the small UCLA CRO system, a wide water recovery range of 10 to up to 73 percent was feasible, depending on the feed salinity (Figure 24). The upper recovery limit is lower at higher salinity and was determined, for example, to be only as high as 37 percent at feed salinity of 11,000 mg/L total dissolved solids (TDS). The source water was ultrafiltered coastal seawater (Naval Base Ventura County, Port Hueneme, California). Salinity was varied via dilutions using RO permeate generated by the UCLA COM2RO desalination system. The shaded vertical rectangular region indicates the range of recovery achievable under steady state RO operation, with higher recovery attainable by operating the system in CRO operational mode. At seawater salinity of 35,000 mg/L, it was more practical to operate in steady state mode at the baseline water recovery of 10 percent due to the high feed osmotic pressure.

Cycle duration decreases with increasing feed water salinity as the osmotic pressure approaches closer to the system's upper limit. Source water: Ulftrafiltered coastal seawater (NBVC, Port Hueneme, California). Salinity was varied via dilutions using RO permeate generated by a separate UCLA RO desalination system operating at a recovery level of 38.6 percent at a permeate production rate of 18,000 GPD (Gao et al. 2013). The implication of operational flexibility on the energy footprint for a practical system in CRO is depicted in Figure 24, showing the specific energy consumption (SEC = energy consumption/product water volume). Only a moderate increase (≤20 percent) in energy footprint was observed with increased water recovery over the highest range of 10 to 73 percent (Figure 24). Clearly, a single CRO system platform can be designed to desalt seawater optimally at the baseline water recovery. Unlike conventional RO systems, that same CRO system can also operate at high recovery when treating low salinity, contaminated water, or brackish water.

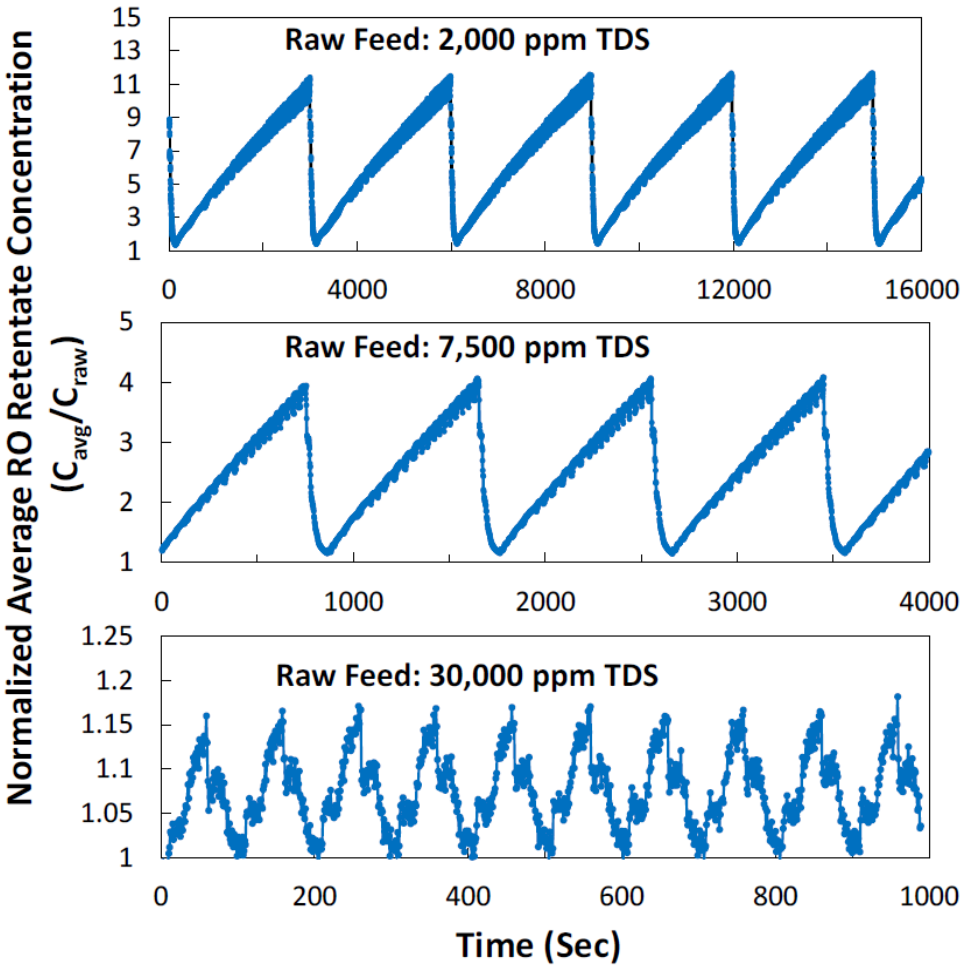

Figure 20. RO concentrate salinity (normalized with respect to raw feed water salinity) in a CRO operation.

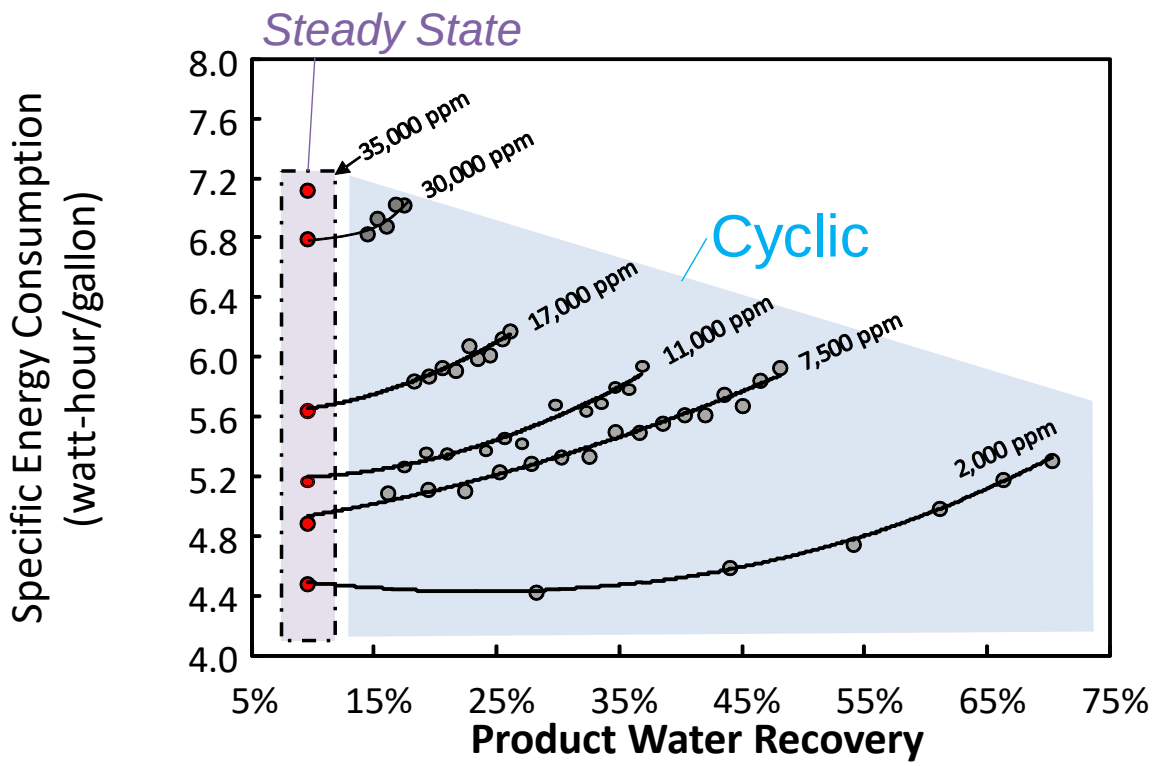

Figure 21. Energy consumption of desalting with a CRO system at various levels of raw feed water salinity and product water recovery measured in parts per million (ppm).

5. References

Bartman, A.R., P.D. Christofides, and Y. Cohen, 2009 (non-linear). Nonlinear Model-Based Control of an Experimental Reverse-Osmosis Water Desalination System. Ind. Eng. Chem. Res., 48(13): p. 6126-6136.

Bartman, A.R., et al., 2009 (feed-flow). Model-predictive control of feed flow reversal in a reverse osmosis desalination process. J. Proc. Control, 19(3): p. 433-442.

Bartman, A.R., et al., 2010. Minimizing energy consumption in reverse osmosis membrane desalination using optimization-based control. J. Proc. Control, 20(10): p. 1261-1269.

Bratt, R.I., 1989. Method and apparatus for fluid treatment by reverse osmosis. US Patent No. 4,814,086 A.

Camacho, L.M., et al., 2013. Advances in Membrane Distillation for Water Desalination and Purification Applications. Water. 5: p. 94-196.

Davies, P.A., 2011. A solar-powered reverse osmosis system for high recovery of freshwater from saline groundwater. Desalination. 271(1–3): p. 72-79.

Efraty, A., 2012. Closed circuit desalination series no-3: high recovery low energy desalination of brackish water by a new two-mode consecutive sequential method. Desalination and Water Treatment, 2012. 42(1-3): p. 256-261.

Efraty, A., 2016. CCD series no-19: The lowest energy prospects for SWRO through single-element modules under plug-flow and closed-circuit desalination conditions, Desalination and Water Treatment.

Efraty, A., R.N. Barak, and Z. Gal, 2011. Closed circuit desalination—a new low energy high recovery technology without energy recovery. Desalination and Water Treatment.
31(1-3): p. 95-101.

Gao, L., et al., 2013. Energy-optimal control of RO desalination. Industrial & Engineering Chemistry Research.

Ghermandi, A. and R. Messalem, 2009. Solar-driven desalination with reverse osmosis: the state of the art. Desalination and Water Treatment. 7: p. 285-296.

GE Global Research, 2006. Integrated wind energy/desalination system. In Subcontract Report NREL/SR-500-39485. National Renewable Energy Laboratory.

Greenlee, L.F., et al., 2009. Reverse osmosis desalination: water sources, technology, and today's challenges. Water Research. 43(9): p. 2317-2348.

Gray, S.R., et al., 2011. Seawater use and desalination technology.

Levenspiel, O., 1996. Chemical Reactor Omnibook, Chap. 68, OSU Bookstores, Corvallis, OR 97339.

Lin, S. and M. Elimelech, 2015. Staged reverse osmosis operation: Configurations, energy efficiency, and application potential. Desalination. 366(0): p. 9-14.

McCool, B.C., et al., 2010. Feasibility of reverse osmosis desalination of brackish agricultural drainage water in the San Joaquin Valley. Desalination. 261(3): p. 240-250.

McFall, C.W., et al., 2008. Control and monitoring of a high recovery reverse osmosis desalination process. Ind. & Eng. Chem. Res. 47(17): p. 6698-6710.

Qiu, T.Y. and P.A. Davies, 2012 (Batch). Longitudinal dispersion in spiral wound RO modules and its effect on the performance of batch mode RO operations. Desalination. 288: p. 1-7. https://doi.org/10.1016/j.desal.2011.11.054

Qiu, T.Y and P.A. Davies, 2012 (Configurations). Comparison of Configurations for High-Recovery Inland Desalination Systems. Water, 4(3), 690-706; doi:10.3390/w4030690

Qiu, T.Y., O.N. Igobo, and P.A. Davies, 2012. DesaLink: solar powered desalination of brackish groundwater giving high output and high recovery. Desalination and Water Treatment, 51(4-6): p. 1279-1289.

Rahardianto, A., et al., 2006. Diagnostic characterization of gypsum scale formation and control in RO membrane desalination of brackish water. Journal of Membrane Science, 279(1): p. 655-668.

Rahardianto, A., et al., 2007. High recovery membrane desalting of low-salinity brackish water: Integration of accelerated precipitation softening with membrane RO. Journal of Membrane Science, 289(1): p. 123-137.

Shaffer, D.L., et al., 2014. Forward osmosis: Where are we now? Desalination, 356: p. 271-284.

Stover, R., 2012. Evaluation of closed circuit reverse osmosis for water reuse. Proc. 27th Annual Water Reuse Symp., Hollywood, FL, USA, September, Water Reuse Association, 2012: p. Paper B4-2.

Stover, R.L., 2013. Industrial and brackish water treatment with closed circuit reverse osmosis. Desalination and Water Treatment, 51(4-6): p. 1124-1130.

Szucz, L. and A. Szucs, 1991. Method and apparatus for treating fluids containing foreign materials by membrane filter equipment. US Patent No. 4,983,301 A.

Thompson, J., et al., 2013. Rapid field assessment of RO desalination of brackish agricultural drainage water. Water Research, 47(8): p. 2649-2660.

Warsinger, D.M., et al., 2016. Energy efficiency of batch and semi-batch (CCRO) reverse osmosis desalination. Water Research, 106: p. 272-282.

Zhu, A., P.D. Christofides, and Y. Cohen, 2009. Effect of Thermodynamic Restriction on Energy Cost Optimization of RO Membrane Water Desalination. Ind. & Eng. Chem. Res., 2009. 48: p. 6010-6021.

Zhu, A., et al., 2010. Reverse osmosis desalination with high permeability membranes—cost optimization and research needs. Desalination and Water Treatment, 15(1-3): p. 256-266.